Use of an Airborne Imaging Spectrometer as a Transfer Standard for Atmospheric Correction of SPOT- HRG Data

Debajyoti Bhowmick
March 2009

Course Title:	Geo-Information Science and Earth Observation for Environmental Modelling and Management
Level:	Master of Science (Msc)
Course Duration:	September 2007 - March 2009
Consortium partners:	University of Southampton (UK) Lund University (Sweden) University of Warsaw (Poland) International Institute for Geo-Information Science and Earth Observation (ITC) (The Netherlands)
GEM thesis number:	2007-01

Use of an Airborne Imaging Spectrometer as a Transfer Standard for Atmospheric Correction of SPOT- HRG Data

by

Debajyoti Bhowmick

Thesis submitted to the International Institute for Geo-information Science and Earth Observation in partial fulfilment of the requirements for the degree of Master of Science in Geo-information Science and Earth Observation for Environmental Modelling and Management

Thesis Assessment Board

Chairman:	Prof. Dr. Ir. Alfred Stein. ITC, The Netherlands.
External examiner:	Prof. Petter Pilesjö. Lund University, Sweden.
Internal examiner:	Dr. Ir. C.A.J.M. Kees de Bie. ITC, The Netherlands.
First supervisor:	Prof. Dr. E. J. Milton. University of Southampton, UK.
Second supervisor:	Dr. Nicholas Hamm. ITC, The Netherlands.

ITC International Institute for Geo-Information Science and Earth Observation
Enschede, The Netherlands

Disclaimer

This document describes work undertaken as part of a programme of study at the International Institute for Geo-information Science and Earth Observation. All views and opinions expressed therein remain the sole responsibility of the author, and do not necessarily represent those of the institute.

Abstract

Earth Observation (EO) data products are required for environmental monitoring and for use in various ecosystem and climatological models that are essential for the advance of Earth system science in securing our planet's future. They are often used in combination with *in-situ* measurements for long term monitoring and modelling. To have confidence in such remotely sensed data in accurately estimating geo-bio-physical parameters, they need to be validated and quality assured. This requires establishing relationship between field measurements and imagery through up-scaling and data aggregation. This up-scaling is non-trivial when the effect of the atmosphere and the very different scales are considered. For example, surface reflectance are scattered and absorbed by the atmosphere before reaching the sensor placed within or at the top-of-atmosphere (TOA). In order to address such issues, this research uses an imaging spectrometer as a transfer standard to account for the effect of atmosphere between field measurements taken on the ground to that measured by a high resolution satellite sensor placed at TOA. Specim AISA-Eagle imaging spectrometer was used as the transfer standard and SPOT-HRG as the high resolution satellite data. All data were obtained as part of the NCAVEO 2006 field campaign. The objective was to use the imaging spectrometer as a transfer standard for atmospheric correction of SPOT-HRG data in order to provide a validated, quality assured data product.

Imaging spectrometers in hyperspectral mode have the capability of resolving the intensity of minor atmospheric absorption features and scattering curve, allowing correction of spectra to values of reflectance (Clark *et al.* 2002). Calibration quality and radiometric linearity of the Eagle sensor was checked with the NERC-CASI-2 sensor, taken to be the standard in this research. A hybrid atmospheric correction method known as the RTGC (USGS) was applied on the Eagle data to obtain a fine resolution reflectance map. It was then validated using two approaches, (i) direct validation with measured ground targets and (ii) indirect validation with an independent reflectance map produced from the EA-CASI-3 sensor. Direct validation agreed to about within ±2 units of absolute reflectance and indirect validation agreed to about ±1.5 units. The Eagle reflectance map was then used to atmospherically correct the SPOT-HRG data using the ELM model to produce the SPOT reflectance map. It was then validated with the Eagle reflectance map and compared with another independent SPOT reflectance map. The results from this research established the potential use of the Eagle imaging spectrometer as a transfer standard in atmospheric correction of SPOT-HRG in providing accurate, validated and quality assured data, which is traceable with known uncertainty.

Acknowledgements

First and foremost I would like to express my heartfelt gratitude to the European Union and the Erasmus Mundus programme for awarding me with the scholarship and the life time experience of travelling and studying in some of the finest institutes of the world in the true spirit of the theologian and humanist Desiderius Erasmus.

I am grateful to all my teachers from University of Southampton, Lund University, University of Warsaw and ITC for not only bestowing precious knowledge but also for continuous support and encouragement. My gratitude to the country and course coordinators of GEM programme: Prof. Terry Dawson, Prof. Petter Pilesjo, Prof. Katarzyna Dąbrowska-Zielińska, Prof. Andrew Skidmore and to Andre Kooiman who was always there to encourage and support us in every way possible.

I am grateful to my supervisors, Prof. E. J. Milton from University of Southampton and Dr. Nicholas Hamm from ITC for their continuous support, advice and guidance. I much appreciate the critical assessment from Dr. Hamm helping me in my endeavour in scientific experience. Prof. Milton has not only been my guide but my mentor as well. I owe to him my interest in the field of "Cal-Val", for accepting me as his student and encouraging me to pursue my thesis in the field of my choice. It has been my greatest pleasure and an honour to have worked along with him. I have gained much more than only scientific knowledge from both my supervisors.

Sincere thanks to Gary Llewellyn, the Science Coordinator for NERC-ARSF for sharing valuable insights and thoughts with me.

Special thanks to Ms. Steff Webb, Ms. Eva Kovacs, Ms Jorein Terlouw and Ms Erna Waayer for their support, hospitality and managing all our problems with a smile.

My admiration goes to all my fellow classmates who have been my friend and extended family in these last 18 months. I also thank my friends from all the countries within and beyond Europe with whom I was fortunate enough to meet. It was a pleasure to live, learn and share views with them. I have truly cherished the time spent.

Finally, my deepest gratitude goes to my parents, my sister and her family. They have been a source of inspiration and encouragement all along. Nothing gives me more pleasure than to dedicate this work of mine to my parents.

Table of contents

List of figures

List of tables

Abbreviations

AATSR	Advanced Along Track Scanning Radiometer.
AREONET	Aerosol Robotic Network
AOT	Aerosol Optical Thickness
ARSF	Airborne Research and Survey Facility
BRDF	Bidirectional Distribution Reflectance Function
CCD	Charged Couple Device
CCRS	Canada Centre for Remote Sensing
CEOS	Committee on Earth Observation Satellites
CFARR	Chilbolton Facility for Atmospheric and Radio Research
CNES	Centre National d'études Spatiales
CASI	Compact Airborne Spectrographic Imager
CASI-2	CASI sensor owned and operated by NERC
CASI-3	CASI sensor owned and operated by Environment Agency
DDV	Dense Dark Vegetation
DN	Digital numbers
DLR	German Aerospace Centre
EO	Earth Observation
EM	Electromagnetic
EMS	Electromagnetic spectrum
ELM	Empirical Line Method
FOV	Field of View
FWHM	Full Width at Half Maximum
HRG	High Geometric Resolution
HCRF	Hemispherical Conical Reflectance Function
IAR	Internal Average Reflectance
INRA	Institut National de Recherche Agronomique
LiDAR	Light Detection and Ranging.
LUT	Look Up Table
MERIS	Medium Resolution Imaging Spectrometer
MISR	Multi-angle Imaging SpectroRadiometer
MODIS	Moderate Resolution Imaging Spectroradiometer
NASA	National Aeronautics and Space Administration
NCAVEO	Network for Calibration and Validation of EO data
NEODC	NERC Earth Observation Data Centre
NERC	Natural Environment Research Council
NIR	Near infra-Red
ROI	Region-of Interest

RS	Remote Sensing
RT	Radiative Transfer
RTGC	Radiative Transfer Ground Calibration
SPOT	Syste`me Probatoire d'Observation de la Terre
STFC	Services and Technology Facilities Council
TOA	Top-of-Atmosphere
UK	United Kingdom
US EPA	United States Environmental Protection Agency
USGS	United States Geological Survey
VALERI	Validation of Land European Remote Sensing Instruments
VIS	Visible
WGCV	Working Group on Calibration and Validation

1. Introduction

1.1. Scientific Context

Remote sensing (RS) is uniquely suited to monitoring the Earth at a global scale. No other surveying method is equipped to measure at such scale and estimate the geo-bio-physical parameters, so important for understanding and securing our planet's future. The communities of researchers interested in the carbon cycle, ecosystem and climate modelling are increasingly interested in measuring "Essential Climatic Variables" (ESA, 2004) which are representative of specific biomes, in order to improve Earth system models at global scale. These variables act as indicators and their accurate measurement would help in understanding global functioning, carbon cycle and vegetation dynamics of the Earth (ESA, 2004). One fundamental constraint within this existing framework is that observations accurate enough to allow parameterisations of such models are only available at a much local spatial scale. On a global scale however, a significant source of error lies in properties estimated from coarse spatial resolution data (Strahler, 2006). Because biosphere parameters determined through field measurements do not represent the appropriate scale, they are therefore inadequate to be used directly in global models. Environmental change metrics at global scale can be very subtle and with the increasing need for accurate parameterisations of global models, there lies a clear knowledge gap between what is known empirically through local measurements and the abstractions inherent in parameterisation used in global models (ESA, 2004).

Establishing relationship between field measurements and imagery is known as up-scaling (Morisette *et al.* 2006). Remote sensing can complement field investigations, offering capability to address spatial scaling issues, characterising environment and improving the parameterisations in models where details of individual processes cannot be explicitly represented. This requires observation to be acquired at appropriate spatial, temporal, spectral and angular resolutions. Even with sufficient temporal resolution and capability of global coverage coarse resolution satellites such as MODIS, MERIS, MISR, AATSR (Strahler *et al.* 2006) are inadequate to characterise spatial variability and non-linearity of biosphere process owing to limited spectral, spatial and angular resolutions (Plotter *et al.* 2003). High accuracy spectro-radiometric measurements representating spatial variability and non-linearity of biosphere process can be used in bridging the gap between observations

made at field and global satellite data by the use of transfer functions. This concept is central to some of the most ambitious and forward-looking research programmes in global RS (e.g. VALERI, BigFoot, CEOS WGCV/LPV, MODIS cal/val, CCRS, US EPA and many others). Most groups use high spatial resolution images often in combination with geostatistical methods as transfer functions to scale up local field measurements to global datasets (Morisette *et al.* 2006; Strahler *et al.* 2006; http://lpvs.gsfc.nasa.gov/; http://landval.gsfc.nasa.gov/).

Teillet *et al*. (2004) in one of their reports to the Committee on Earth Observation Satellites – Working Group on Calibration and Validation (CEOS-WGCV) mentioned that monitoring by satellite sensors combined with networks of *in-situ* observations is the only feasible approach for measurement and long-term monitoring of terrestrial parameters. The challenge lies in providing reliable RS data to the users and ensuring that measurements and methods yield self-consistent and accurate geo-bio-physical parameters made from different sensors under varying observation conditions using dissimilar methodologies. Data standardisation and product validation are critical aspects of Earth Observations (EO) data if they are to reflect terrestrial processes as they really are, and not compromised by sensor and data processing artefacts. With the advent of new, varied and advanced sensors also comes the responsibility to deliver products, brought to the same standard of physical units, calibrated to the same standard and validated with field measurements if they are to contribute to the much needed global products (Teillet *et al.* 2001). Two important issues need to be addressed in data validation and up-scaling: (i) the atmospheric effect on RS data within the atmosphere and (ii) accounting for different spatial resolution between sensors for data aggregation generally at the Top-of-Atmosphere (TOA). Atmospheric correction assumes knowledge of the first transfer function in removing the atmospheric influence; statistical computation assumes knowledge of the second transfer function in accounting for spatial resolution in this whole framework of up-scaling and data aggregation for deriving validated global data products.

Airborne imaging spectrometers have very high spatial and spectral resolution, and so have tremendous potential to act as transfer standards addressing the atmospheric transfer function in the up-scaling process from field measurements to high resolution satellite data at TOA. The second transfer function at TOA which is beyond the scope of the present study deals with transferability of measured radiance amongst varying spatial resolution of sensors through rigorous statistical computations. The final validated product can be used for any quantitative analysis with much confidence. This research aims to evaluate the newly introduced AISA-

Eagle imaging spectrometer in the UK as a potential transfer standard for atmospheric correction of SPOT-HRG data. The process can be replicated in future to similar scientific and operational endeavours.

1.2. Why atmospherically correct SPOT?

SPOT-5 is the fifth satellite in the SPOT (Syste`me Probatoire d'Observation de la Terre) series designed by Centre National d'études Spatiales (CNES) of France with partnership from Belgium and Sweden. The on-board High Geometric Resolution (HRG) sensor of SPOT-5 offers a ground spatial resolution of 10 metres in multispectral mode in green, red and near infra-red (NIR) bands of the electromagnetic spectrum. (Appendix-A. SPOT-5 HRG specifications). Within the European context, SPOT is probably the most widely used satellite sensing system as it offers an effective ground resolution small enough to resolve the typical field sizes. The Validation of Land European Remote Sensing Instruments (VALERI) project initiated in 2000 supported mainly by CNES and the Institut National de Recherche Agronomique (INRA), has focused on the development of an effective methodology to generate high spatial resolution maps of biophysical variables from satellites and the use of those maps for the validation of moderate-resolution global products. SPOT was chosen as the main high resolution EO data before comparing with moderate resolution products could be carried out (Morisette *et al*. 2006). The Ordnance Survey has also identified SPOT as the most suitable system for monitoring land cover change in the UK (Anandakumar, 2008). Demand for better land surface characterisation using remotely sensed data is ever increasing, resulting in improved models and algorithms. These in turn require accurately derived products of the surface material from space borne imageries. This mutually benefiting and reinforcing cycle, challenges how accurately physically meaningful data can be extracted from satellite imageries and SPOT occupies an important role in this segment of high resolution space borne RS sensor.

1.3. Research Problem

There is an acute need for EO data products in combination with *in-situ* measurements for up-scaling and validation to provide quality data product for Earth system science and long-term modelling and monitoring. Up-scaling field data and validating EO product is crucial when the effects of atmosphere are considered between measurements taken on the ground which may have a spatial support of few centimetres to a pixel size of kilometres taken from a space sensor. Addressing such a problem within the scope of this research, required downscaling of the project to look at how a high resolution SPOT-HRG data can be validated by up-scaling field

measurement using an Eagle imaging sensor as a transfer standard. Often atmospheric correction of satellite products such as SPOT are achieved using an empirical transfer function which assumes that the atmosphere remains constant over the site which is rarely the case (Gao *et al*. 1991 in Smith and Milton, 1999). Therefore there is need for a transfer standard which can accurately account for the local scale spatial variability in the atmosphere. Specim AISA-Eagle is an imaging spectrometer relatively new in the United Kingdom (UK), and therefore its quality as a potential transfer standard is unknown. It is quite similar to the Itres Compact Airborne Spectrographic Imager (CASI-2) sensor which has been flown for about twenty years by the UK Natural Environment Research Council's Airborne Research and Survey Facility (NERC-ARSF) (Appendix-B. CASI-2 specification). Calibration of the CASI-2 is routinely checked in the laboratory and the instrument is subjected to annual re-calibration by the manufacturer, Itres Instruments (Riedmann, 2003). Within this scaled down framework, the research problem seeks to evaluate the Specim Aisa-Eagle as a potential transfer standard in atmospheric correction of SPOT-HRG data to provide a validated product. Discussion with Gary Llewellyn, the Science Coordinator for NERC-ARSF, revealed that NERC intends to retire the CASI-2 sensor after the last flying season in 2008. (Llewellyn, pers. Comm. Nov, 2008). With CASI-2 being phased out and AISA-Eagle becoming the next default sensor for the NERC-ARSF an evaluation of the AISA-Eagle sensor and an assessment of its potential as a transfer standard to atmospherically correct SPOT–HRG would be of great practical importance to users of the ARSF facility.

1.4. Novelty and Rationale of the research

Much effort and millions of euro are spent by mapping agencies all over Europe for retrieving accurate, reliable and lasting data products from satellite imageries with varied resolutions (spatial, spectral, temporal and radiometric). It is still an evolving subject and the 'best practice' is not yet established limiting its operational use (www.ncaveo.ac.uk). This research addresses the importance of an imaging spectrometer as a transfer standard for atmospheric correction of SPOT-HRG data in order to provide validated and quality assured product. The data were collected as part of Network for Calibration and Validation of EO data (NCAVEO) field campaign 2006 in Chilbolton, UK (see Chapter-3). Figure.1-1 describes the scope of the work.

The advantage of using the Specim AISA-Eagle sensor lies in its very high nominal ground resolution (1m) and operating capability in the visible (VIS) to near infra-red (NIR) region of the electromagnetic spectrum (EMS) (~ 0.4 – 0.97 µm), acquiring data in 244 contiguous bands providing rich data source in the spatial and spectral

domain. (Appendix-C. Specim AISA-Eagle specification). This makes the sensor ideal for simulating most civil Earth Observation satellite sensors operating in the VIS/NIR region.

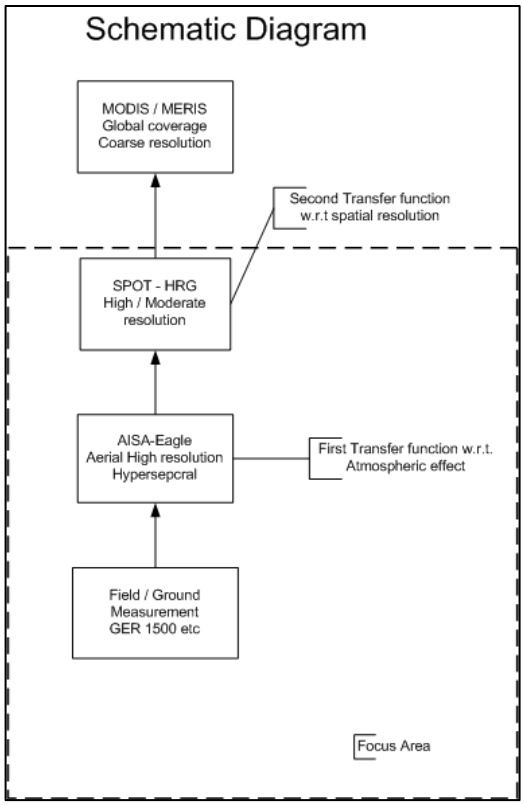

Figure 1-1 Schematic diagram of transfer function with dash bordered being the focus area of the study

The research would require evaluation of the Eagle sensor compared to the known calibration quality of the CASI-2 sensor which was taken to be the standard in this study in establishing its potential as a transfer standard. This would deliver practical result of immediate benefit to the many scientists wishing to use the Eagle data collected as part of the NCAVEO 2006 field campaign and potential use of it as a transfer standard in atmospheric correction would provide much value addition for such scientific application. This research has a significant scientific and practical contribution towards the larger realisation of offering calibrated and validated EO data products to users who need them the most.

1.5. General Objective

Potential use of the AISA-Eagle imaging spectrometer as a transfer standard in atmospheric correction of SPOT-HRG data by applying the Empirical Line Method (ELM) using the reflectance map generated from the spectrometer.

1.6. Research Questions

Specific Objective	Research Questions
Evaluate AISA-Eagle sensor compared to CASI-2 sensor.	i. How does the calibration quality of Eagle compare to CASI-2 sensor? ii. What is the radiometric response of the Eagle sensor based on CASI-2 sensor?
Create an accurate reflectance map of the NCAVEO-Chilbolton validation site	iii. Does Eagle data produce an accurate reflectance map for use in upscaling to SPOT-HRG data? iv. Can the Eagle reflectance map be used to identify suitable calibration targets for SPOT considering: - size in relation to SPOT pixels? - range of reflectance in each band? - stable composition ?
Atmospheric correction of SPOT HRG data using Empirical Line Method (ELM) using the Eagle reflectance map.	v. Can the Eagle reflectance map be used to atmospherically correct SPOT-HRG to provide a validated and calibrated data product?

1.7. Hypothesis

- H_0 =Radiance measured from Eagle and CASI-2 under identical operating conditions are similar.
- H_a = Radiance measured from Eagle and CASI-2 under identical operating conditions are significantly different.

1.8. Research Stages

1) The first stage involved requiring necessary permissions and formalities to access the NCAVEO 2006 field campaign data from the UK NERC Earth Observation Data Centre (NEODC). Required data were downloaded which primarily included data from the Specim AISA-Eagle, NERC-CASI, and the SPOT- HRG along with the field measured spectra. Ground targets were indentified from the flight lines and geometrically corrected using the AZGCORR software. The input in this process was Level-1b and the rectified output was Level-3a as per National Aeronautics and Space Administration (NASA) standard.

2) The second stage focused on the process development. This involved evaluating Eagle sensor compared to CASI-2, creating accurate reflectance map of validation site and correcting the SPOT-HRG data from it using the Empirical Line Method (ELM) model. At first sensor calibration and radiometric linearity of the Eagle sensor was evaluated against CASI-2. Then using RTGC (USGS) hybrid method (see Chapter-3) reflectance map from Eagle data was generated and validated with field measurements. Suitable ground targets were identified from the Eagle reflectance map and using the ELM model the SPOT-HRG data was atmospherically corrected. It was then validated with the Eagle reflectance map and compared with an independent reflectance map of the same SPOT data.

3) The final stage involved abstracting information and drawing conclusions and recommendations from the research. Advantages and limitations of the approach were discussed within the scope of scientific and operational domain.

2. Literature Review

2.1. Atmosphere: Its effect and how it is characterised.

The surface signals are modulated by the Earth's atmosphere twice. It affects the distribution of incoming solar radiation at surface, related to surface reflectance and further scattered and absorbed by the atmosphere before reaching the sensor placed within or at the top-of-atmosphere (TOA). The radiance measured by the sensor thus contains information of both the atmosphere and land surface (Liang, 2004) and needs to be corrected for these effects before they can be used either on their own or within a temporal dataset to monitor environmental changes (Karpouzli and Malthus, 2003). The principle of atmospheric correction aims to remove the error sources of atmospheric contribution from the at-sensor radiance spectra from the useful ground-leaving radiance. Effect of aerosol and molecular scattering is stronger at shorter wavelengths of the solar EM spectrum. This increases the apparent surface reflectance over dark surface while aerosol absorption (water vapour, ozone, oxygen) reduces the reflectance of brighter surfaces (Sharma *et al.* 2009). Traditional review of the same can be found in the work of Kaufman (1989).

Airborne imaging spectrometer provides rich information of the surface materials under study. In hyperspectral mode because of their very narrow bandwidth and ultrafine resolution they have the capability of resolving intensity of even minor atmospheric absorption features and scattering curve allowing better correction of RS spectra to values of reflectance (Clark *et al*. 2002). Atmospheric correction is a prerequisite for interpreting surface reflectance (Guanter *et al.* 2007). Experience with field and airborne instrument suggests that, a Full Width at Half Maximum (FWHM) of individual bandwidth of 10nm and a bandwidth of 15nm for contiguous spectral bands are adequate to resolve most of the surface features in the (400nm – 2400nm) spectral range (ESA, 2004). Advanced atmospheric correction algorithms for hyperspectral data lies on a radiative transfer (RT) approach (Adler-Golden *et al.* 1999; Goetz *et al.* 2003; Liang and Fang, 2004; Miesch *et al.* 2005; Miller, 2002; Richter and Schlaepfer, 2002; Staenz *et al.* 2002) to invert the surface reflectance from registered at-sensor radiance (Guanter *et al.* 2007).

2.2. Difficulties in atmospheric correction

The atmosphere is one of the uncertain variables involved in the process of remote sensing. This is because, of its very dynamic nature and the potential to vary between different and extreme weather conditions. This is particularly true for temperate regions noted for their unpredictable weather conditions such as in major parts of Europe. In terms of atmospheric correction of RS data, except for some dedicated field experiments, *in-situ* measurements of active atmospheric constituents such as aerosols and water-vapour which mostly influence the approach are rare (Guanter *et al.* 2007). Most atmospheric gases are quite stable in space and time and absorb energy in very narrow spectral range of the EMS (Liang, 2004) and are usually minimised by choosing bands in the atmospheric windows (Kaufman, 1989). In visible part of the spectrum, transmission is affected mainly by molecular scattering formulated by Rayleigh (1871) and ozone absorption. Optical thickness due to molecular scattering (nitrogen and oxygen) depends on pressure level and can be computed for any known elevation, while ozone contribution at 550 nm is quite small and climatologic / geographic average can be taken. This leaves aerosol contribution (scattering and absorption) as one of the most important component which varies strongly in space and time. Aerosol Optical Thickness (AOT) at 550 nm is often used to characterise atmosphere instead of visibility in atmospheric correction process (Richter, 2008).

2.3. Atmospheric correction approaches

The whole sequence of extracting surface reflectance follows some cascading steps. From Digital Numbers (DN) to 'At-Sensor-Radiance' to 'Ground-Leaving-Radiance' and finally to 'surface reflectance' involves accounting for sensor calibration, atmospheric correction and reflectance calibration. This is illustrated in Figure 2-1 below.

Though conceptually calibrating to surface reflectance from radiance is simple, neither model, empirical nor radiative are characterised to precision accuracy (Green *et al*. 1998). The advantage offered by reflectance value extracted from radiance after atmospheric correction is that the calibrated spectra exhibit physical and chemical properties of targets and can be compared with field or laboratory spectra. Therefore maps derived from calibrated surface reflectance offers greater confidence in interpreting the information (Clark *et al*. 2002). Atmospheric correction may broadly be classified into (a) Empirical method and (b) Physically based method involving numerical models which is illustrated in Figure2-2 below:

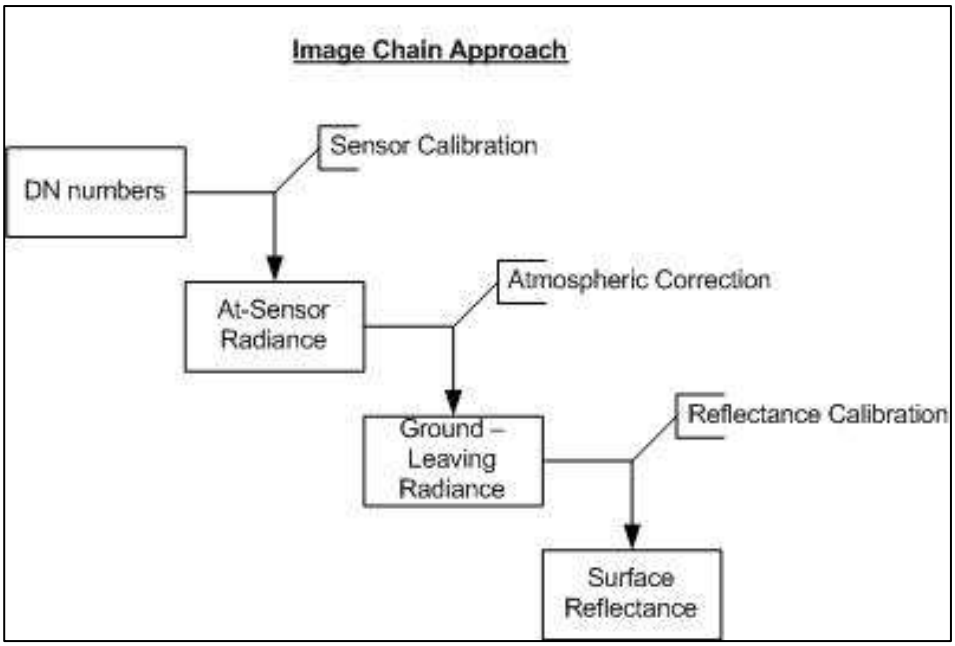

Figure 2-1 Diagram showing the image chain approach

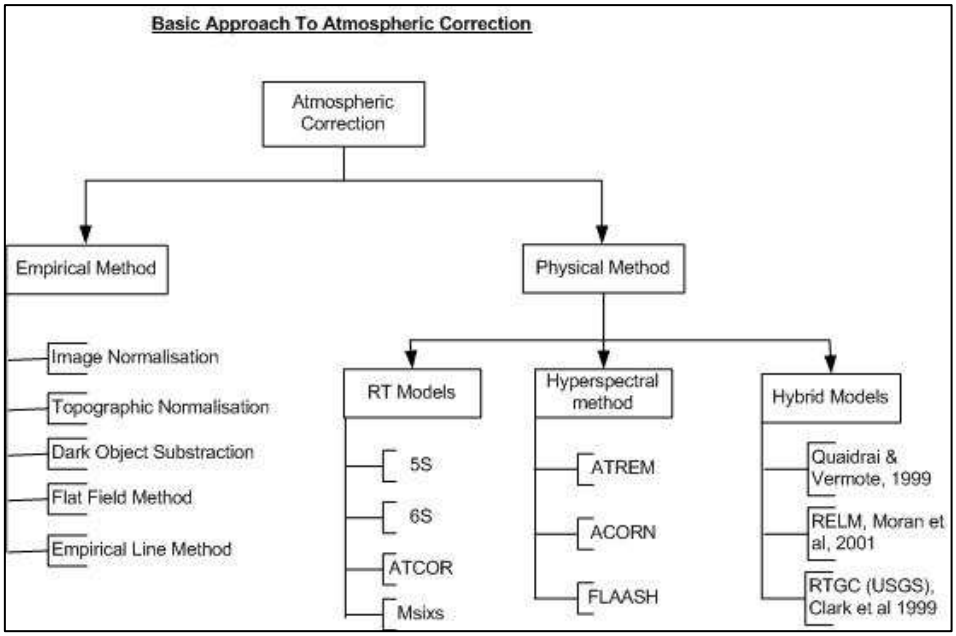

Figure 2-2 Diagram showing atmospheric correction approach.

Appeal of scene derived approach lies in the ability to atmospherically correct RS data without depending on external information or measurements such as with the Internal Average Reflectance (IAR) approach of Kruse (1987). The "Flat Field" correction method (Roberts *et al*. 1986; Carrere and Abrams, 1988) assumes the scene area to be spectrally flat, having near-Lambertian response, temporally stable reflectance and spatially uniform and homogenous. The Dense Dark Vegetation (DDV) approach of Kaufman and Sendra (1988) used dense dark vegetation like coniferous and used it as 2% target in red band. Though these methods are essentially independent of external information, assumptions relied in such methods are often difficult to meet in practice (Clark and King, 1987; Kruse, 1987). The Empirical Line Method (ELM) of Conel *et al*. (1987) requires field measurement of surface reflectance from ground targets of at least one bright and dark target in order to derive additive and multiplicative correction factors. The RS data over the surface targets are linearly regressed against the field-measured reflectance to derive the gain and offset curves which are then applied to the whole image for derivation of surface reflectance of the entire scene. More detailed reviews about advantages and disadvantages of empirical and physically based methods can be found in the works of Roberts *et al*. (1986) and Moran *et al*. (1992).

Physics based radiative transfer models describe the radiative transfer in terms of interaction with gases and particles, interaction with the surface and transmission along a different path upward through the atmosphere to the sensor (Gao *et al.* 1993; Leprieur *et al.* 1995; Zagolski and Gastellu-Etchegorry 1995; Adler-Golden *et al.* 1999; Schlapfer *et al.* 2000 and Qu *et al.* 2000). They describe the solar irradiance function, the absorption and scattering process of atmospheric gases and reflection from surface materials all as a function of the wavelength of EM radiation and the directional angles of sensor and sun with respect to pixels of RS data as they are located on Earth surface. Radiative transfer problem are complex and numerical models use simplified assumptions to achieve reasonable computation times (Karpouzli and Malthus 2003). Though comprehensive and well defined, radiative transfer calibration show residual atmospheric absorption and scattering effect from inadequate definition of solar irradiance function, variation in the source of illumination and simplified assumption of physics that describe atmospheric gaseous absorption. These may result in errors in the calculated reflectance (Clark *et al.* 1993, 1995).

Hybrid approach combines both physical (additive correction factor – estimate of path radiance) and empirical methods (multiplicative correction derived from ground measurement) for atmospheric correction which results in well-calibrated

surface reflectance values near the calibration sites. For example, the Radiative Transfer Ground Calibration (RTGC) method developed by Clark *et al*. (1993, 1995); the Quaidrai and Vermote (1999) method and the Refined Empirical Line Method (RELM) approach by Moran *et al.* (2001).

2.3.1. Empirical Line Method

The Empirical Line Method (ELM) was traditionally performed for atmospheric correction by Conel and Alley (1985); Roberts *et al.* (1986); Conel *et al.* (1987); Farrand *et al.* (1994). The method matches the RS data with the *in-situ* spectra by an equation which can be expressed as:

$REFLECTANCE_k = A_k * BV_k + B_k$

where BV_k is the digital brightness value for a pixel of band k, $REFLECTANCE_k$ equals the *in situ* surface reflectance of the materials within the remote sensor IFOV at a specific wavelength, A_k is a multiplicative term (gain) affecting the BV_k, and B_k is an additive term (offset). The multiplicative term is associated primarily with atmospheric transmittance and instrumental factors, and the additive term deals primarily with atmospheric path radiance and the instrumental offset. The correction is applied band by band and not pixel by pixel (Jensen, 2005). The ELM method assumes that within the image there are one or more targets with different reflectance characteristics encompassing a wide range of reflectance values for each wavelength measured by the sensor (Smith and Milton, 1999).

In its simplest form, this approach can be used with a single target assuming zero reflectance produces zero radiance but can give high error up to 20% of actual value (Freemantle *et al.* 1992). The gain and offset values are derived using simple linear regression using the field measured spectra (Farrand *et al.* 1994). The image DN and reflectance data are equated for each band using the linear regression, thus removing the solar irradiance and the atmospheric path radiance. In a simple model with two targets the four spectra (two from image and two from *in situ*) can be used to implement an empirical line calibration to derive the appropriate gain and offset values (Hadley *et al.*2005). There is evidence that use of more targets allows the parameters of the model between at-sensor radiance and at-surface reflectance to be estimated with greater confidence (Farrand *et al.* 1994; Price *et al.* 1995; Smith and Milton, 1999; Karpouzli and Malthus 2003). Many researchers (e.g. Kruse *et al.* 1990; Ben-Dor *et al.* 1994; Vandermeer, 1994; Dwyer *et al.* 1995, Ferrier and Wadge 1996) have used two calibration targets to generate acceptable calibration but not enough was reported on validation result. There are assumptions associated with ELM which states (a) there is no differences in illumination across the image and hence changes in radiance due to cloud shadowing or topography are ignored,

(b) even though atmospheric constituents such as water vapour can vary greatly over short distances (Gao *et al*. 1991 in Smith and Milton, 199) it assumes the state of atmosphere to be uniform and (c) also assumes Earth surface to be Lambertian while in reality it posses Bidirectional Distribution Reflectance Function (BRDF) properties (Smith and Milton, 1999). Although finding large contrasting homogenous targets might be difficult for image footprints for satellites such as Landsat and SPOT (Karpouzli and Malthus 2003), the relative ease and simple method of ELM attracts scientist to adopt this technique. Moreover if the targets were found to be temporally stable, it is not even necessary for concurrent measurements with data acquisition (Teillet *et al.* 1999; Karpouzli and Malthus, 2003).

2.3.2. Hybrid method – RTGC (USGS)

Though radiative transfer methods are theoretically robust and well defined, nevertheless produce apparent surface reflectance values with residual atmospheric absorption and scattering effects. The Radiative Transfer Ground Calibration (RTGC) method was developed at the United States Geological Survey (USGS) as a hybrid approach for atmospheric correction (Clark *et al.* 1993,1995). The RT model corrects the image based on spectral absorption feature of water vapour while the ground calibration removes the residual errors pertinent to RT approaches (Gao *et al.* 2006). This allows an additive correction factor (an estimate of path radiance) and a multiplicative correction factor derived from the ground measurements of reflectance. In comparison with several methods, Clark *et al.* (1993 and 1995) found RTGC method to give better calibration result with imaging spectrometers. The drawback is increased residual absorption for pixels away from the calibration site and for pixels with different path lengths through the atmosphere caused by a changing scan angle of sensor (Clark *et al.*2002).

2.4. Choice of Ground Targets:

Ground calibration targets play an essential role in atmospheric correction and vicarious calibration. However almost always some assumptions are made about the targets (Anderson and Milton 2006). Therefore there are some considerations in choosing the right ground targets.

1. The calibration targets should be spatially homogenous. It is an area on a scale which can be characterised in the field and by the sensor, where pixel to pixel variation in the reflectance spectra is low. For example, if a site is composed of different pebbles, but both spectrometer and imaging sensor can average many pebbles together, the site is most likely to be acceptable (Clark *et al.* 2002).

2. The calibration target should be both spectrally bland and uniform. Spectrally bland refers to having no strong absorption features in the measured wavelengths. If spectral features are not well characterised it might result in residual spectral features added to all pixels in the final calibrated data. Spectrally uniform refers that the site must not contain different features in the background (Clark *et al.* 2002).
3. A bright target with high reflectance level is preferred. This allows to being more sensitive to multiplicative correction (multiplication factor for each spectral channel) while low reflectance is more sensitive to additive offsets such as atmospheric scattering (Clark *et al.* 2002).
4. The calibration target should be large enough so as to accommodate as many sensor pixels covering the site. Averaging of many spectra allows minimising noise in flight data calibration, though some will always be present. The noise decrease as the square root of the number of pixels averaged (Clark *et al.* 2002).
5. Elevation of target site and study site should be same or similar. This is important because optical thickness due to molecular scattering (nitrogen and oxygen) only depends on pressure level and can be calculated for known ground elevation (Richter, 2008).
6. The calibration target should be temporally stable with near Lambertian response (Anderson and Milton, 2006).

2.5. ATCOR 4:

Atmospheric & topographic correction for wide Field-of-View (FOV) airborne optical scanner data (ATCOR 4) has been developed jointly by the German Aerospace Centre (DLR) and ReSe Application. The suffix 4 refers to the four degrees of freedom (x, y, z and scan angle) and hence ATCOR 4. It employs a large high resolution (monochromatic) atmospheric database, compiled using the "MODerate spectral resolution atmospheric TRANSmittance algorithm and computer model" (MODRAN-4) code employing DISORT, 8stream option (DIScrete Ordinate Radiance Transfer) for computing multiple scattering components of the total path radiance. This can be employed for both small and wide FOV sensors operating in altitudes ranging from 1km - 20 km. For a given sensor and altitude, the corresponding altitude file and the atmospheric database needs to be resampled along with the spectral filter functions for all channels (Richter, 2008).

3. Study area and Data Collection

3.1. Study area

The study area was located in England within Hampshire, south-east of Andover, approximately 45 km north of Southampton (Figure 3-1). The area was 9 km north-south by 6 km east-west, the south-west corner defined by the Ordnance Survey grid reference SU 370360. The site was centred on the Services and Technology Facilities Council (STFC) Chilbolton Facility for Atmospheric and Radio Research (CFARR). CFARR, surrounded by land cover typical of southern England also offered instruments for measuring the atmospheric properties. It also forms part of the Aerosol Robotic Network (AERONET) site measuring AOT and total atmospheric water vapour by Cimel sunphotometer every 15 minutes calibrated to NASA standard (Milton, 2008; www.ncaveo.ac.uk).

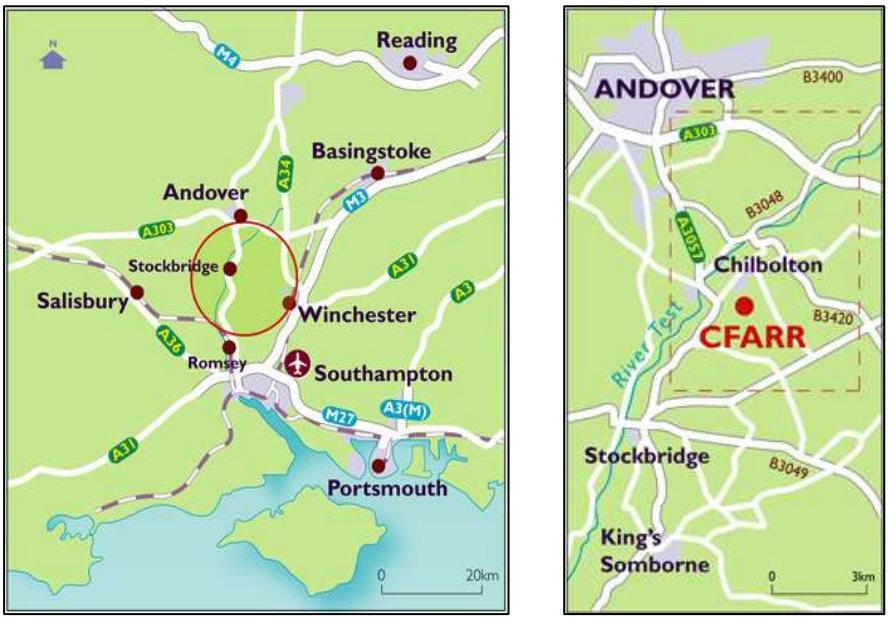

Figure 3-1 Location and extent of study area (Source: www.ncaveo.ac.uk)

3.2. Data Collections

Data used in this study were obtained as part of NCAVEO 2006 field campaign which took place on 17th June, 2006. The campaign involved data collection from seven EO satellites and three aircrafts fitted with hyperspectral sensors, LiDAR and digital survey cameras from a core area of 54 km^2 from 5th to 23rd June 2006 with most effort concentrated around the overpass on 17th June 2006 (Appendix-D. summery of timeline and flight mission). Near-simultaneous field measurements were taken for many datasets to allow for inter-comparison (Milton, 2008). All data were archived at the NERC EO Data Centre (NEODC) and are made available for this research. Key datasets and their brief description are described below in Table 3-1 and details of the independent datasets used for indirect validation are shown in Table 3-2 below.

Table 3-1 Details of key data sets

Date	Data	Key specs	Brief summery
17-06-06	CASI-2 flown by NERC	VNIR 15 bands / 2 m	9 flightlines acquired using an Itres Compact Airborne Spectrographic Imager. Registered to British National Grid using data from on-board sensor.
17-06-06	Specim AISA-Eagle flown by NERC	VNIR 244 bands / 1 m	9 flightlines acquired using Specim AISA-Eagle imaging spectrometer. Registered to British National Grid using data from on-board sensor.
10-06-06	SPOT-5 HRG operated by CNES	VNIR/SWIR 4 bands / 10 m/20m	Half-scene (029/246) centred on 51˚12'N and 1˚27'W acquired on 10th June'06. Registered to the British National Grid using ground control points.
17-06-06	AOT	Every 15 mins	Measurements every 15 minutes from two Cimel CE318-2™ sun photometers, one of which is part of AERONET calibrated to NASA standard ….cont.

Date	Data	Key specs	Brief summery
17-06-06	Field spectra	Asphalt	Reflectance was acquired from the CFARR car park apprx. 3m x 3m using a GER1500
		Concrete	Reflectance was acquired from a fixed tripod near the north-east corner of target using a GER3700, 1 m above the surface with a nominal 3˚ FOV
		Fabric spectra	Reflectance spectra collected from 3 artificial targets (white, grey and black tarpaulin) using contact probe (cp) measurements using an ASD 6408 unit. 10 randomly positioned measurements per quadrant anticlockwise from SE corner.

3.3. Independent data collection for validation

Table 3-2 Independent data sets for validation

Data	Correction method	Source	Brief Summery
Reflectance map from EA-CASI-3 sensor	RTGC (USGS) using ATCOR-4	NCAVEO (2008)	The EA-CASI was flown over the target area shortly before the NERC CASI and Eagle was flown, at a much higher altitude.
Reflectance map from SPOT-HRG	RT using ATCOR-2	Anandakumar, R.M (2008)	The reflectance map of SPOT-HRG was atmospherically corrected using RT method applying ATCOR 2

3.4. Software

1. ENVI image processing software, full version from IIT VIS.
2. Azgcorr and Azexhdf geometric correction software by Azimuth Systems, UK.
3. ATCOR-4 from ReSe Applications Schläpfer
4. SPSS Statistical software from SPSS Inc.
5. HDF Explorer to interrogate metadata.
6. MS Excel from Microsoft Corporation.

4. Methodology

The process of evaluating Eagle sensor as a transfer standard and atmospheric correction of SPOT-HRG involved a few intermediate stages. The whole process flow is illustrated in the following flow-diagrams (Figure 4-1; 4-2; 4-3 and 4-4). It involved three major stages of (i) evaluating the Eagle sensor (ii) creation of an accurate reflectance map and (iii) correction of SPOT-HRG. Figure 4-1 illustrates the overall approach and how they were interlinked with each subsequent stage.

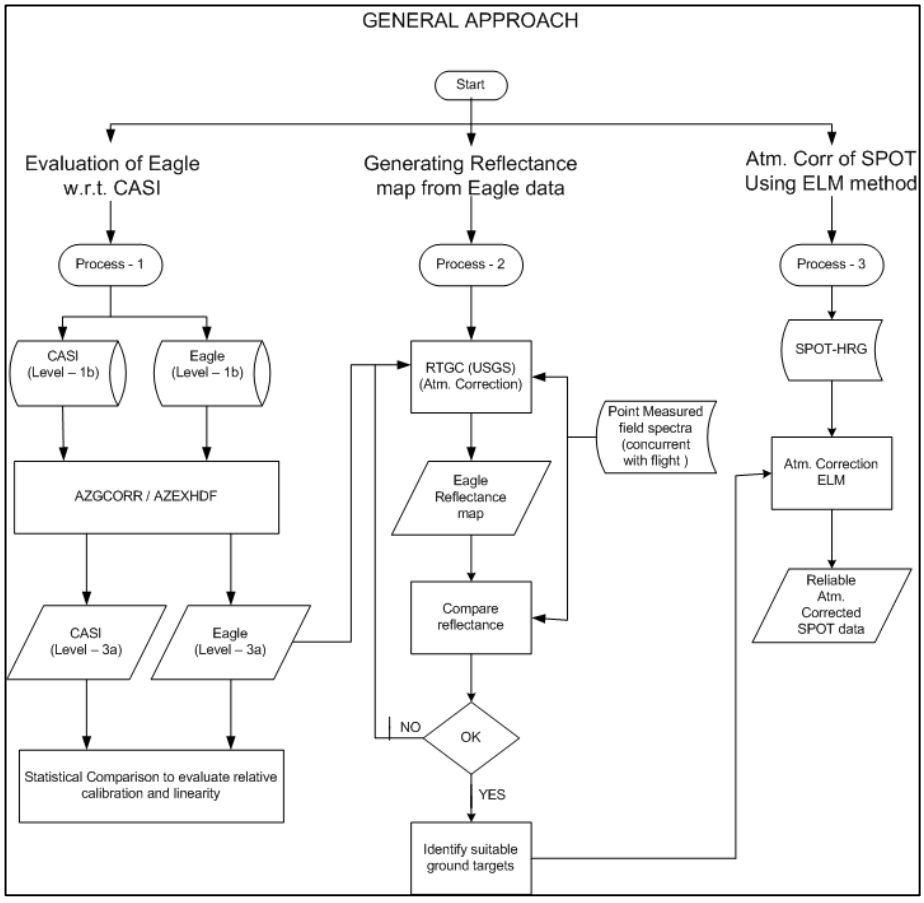

Figure 4-1 Diagram illustrating the general approach for the complete process flow.

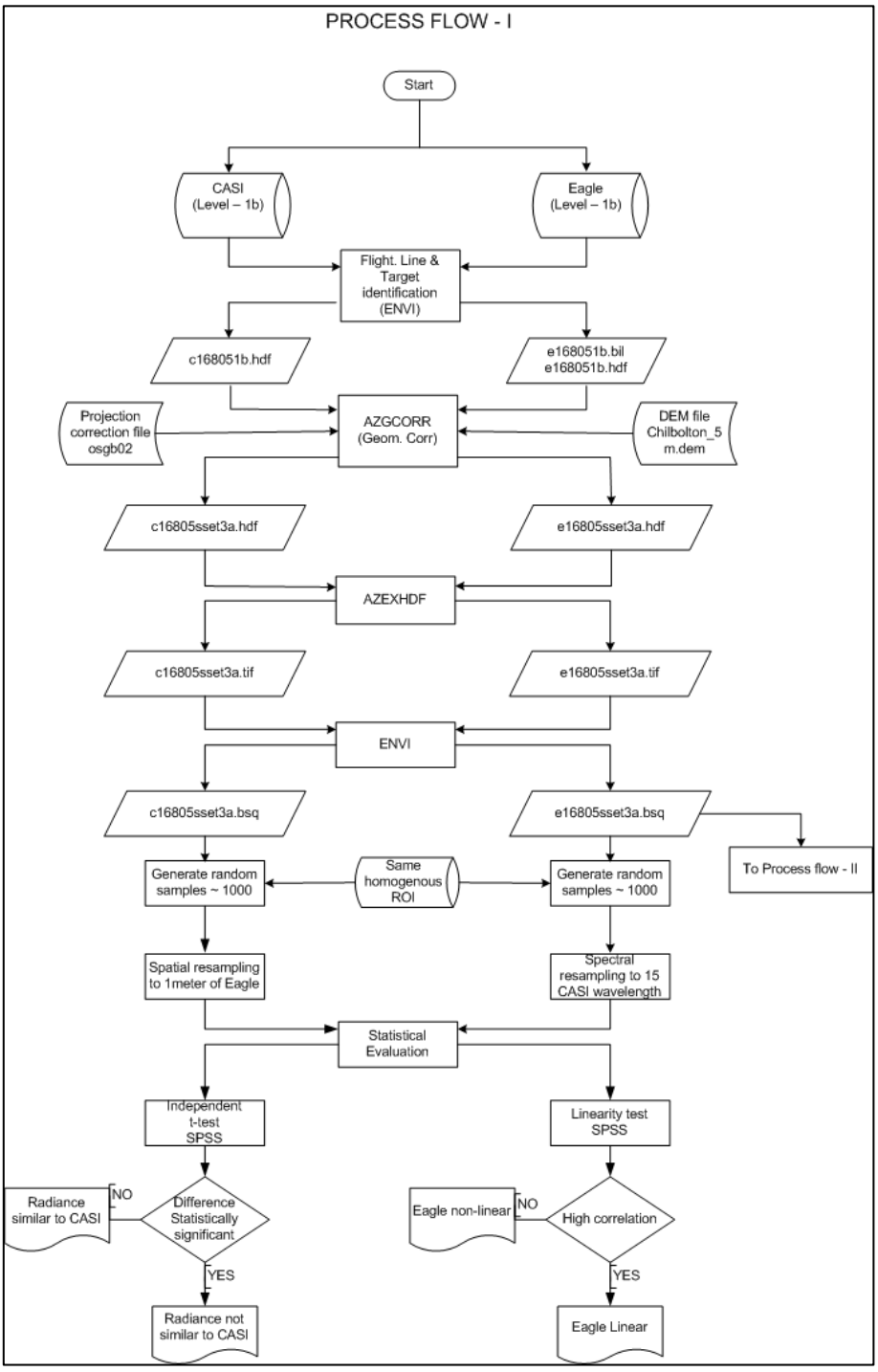

Figure 4-2 Flow diagram illustrating evaluation of Eagle sensor to CASI-2.

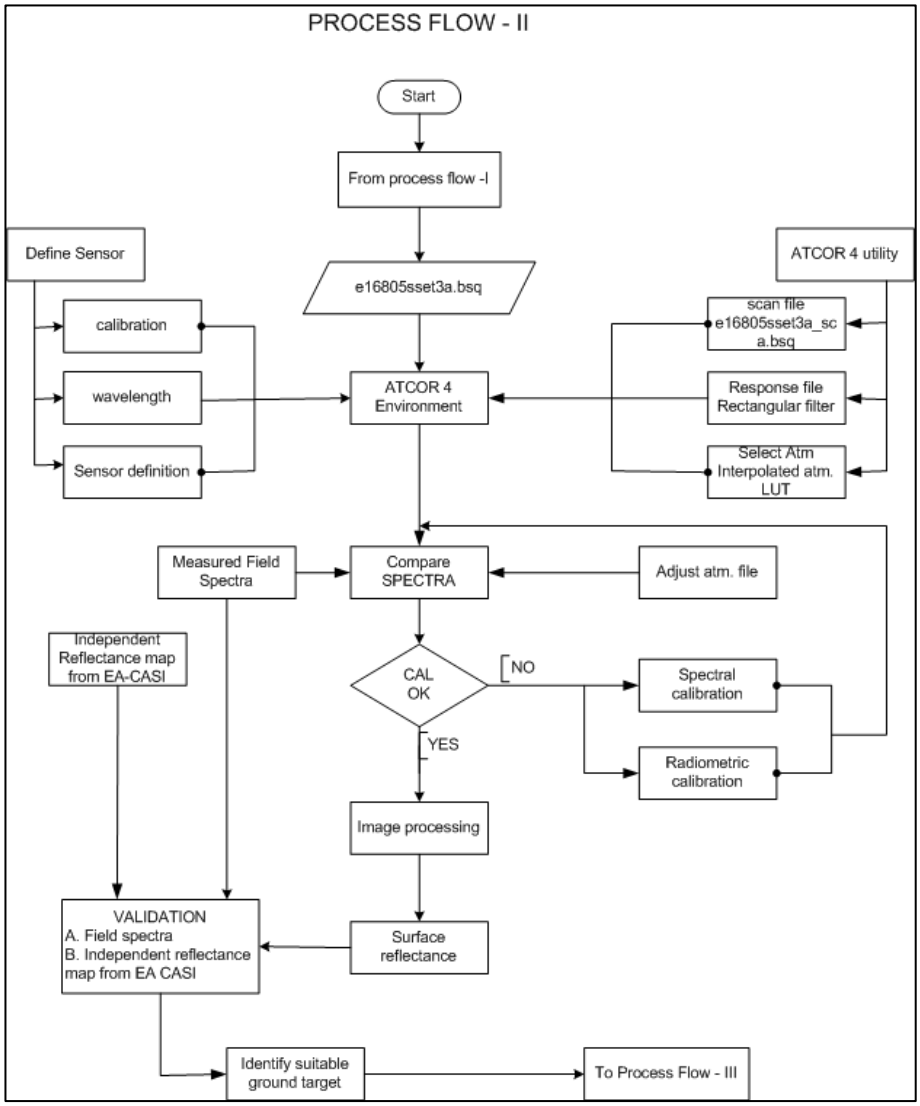

Figure 4-3 Flow diagram illustrating the RTGC (USGS) atmospheric correction procedure using ATCOR 4.

Figure 4-2 describes the process of geometric correction and statistical tests carried out to evaluate Eagle compared to that of CASI-2. Figure 4-3 describes the RTGC (USGS) atmospheric correction of Eagle data and Figure 4-4 describes the ELM correction of SPOT-HRG using the data from the transfer standard.

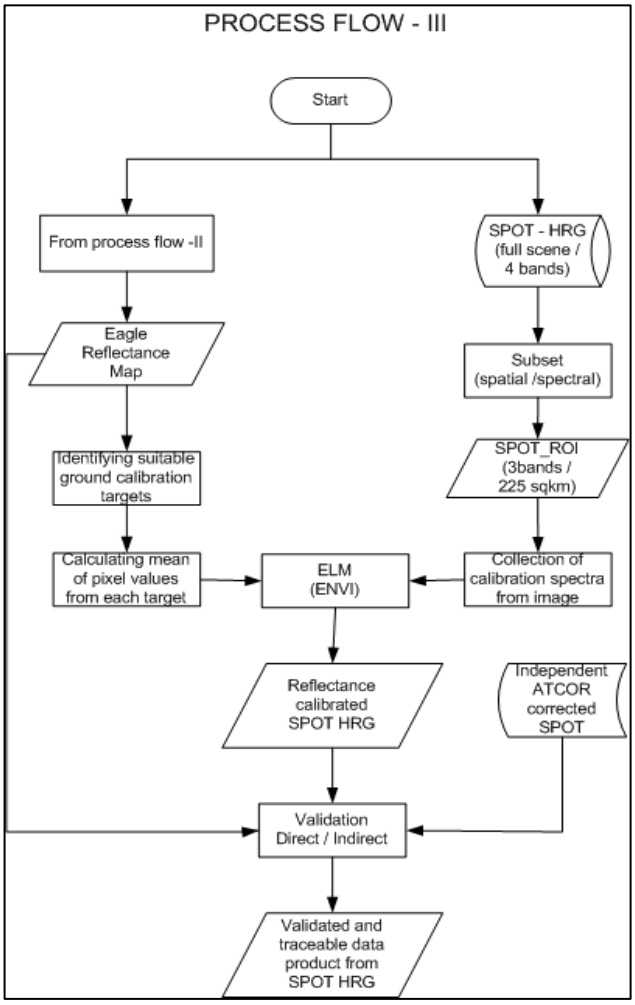

Figure 4-4 Diagram illustrating the ELM of atmospheric correction of SPOT.

4.1. Description of Process Flow - I

As a first step towards evaluating AISA-Eagle's suitability as a transfer standard, its calibration quality and estimate of its detector linearity needed to be assessed. For this purpose Itres Compact Airborne Spectrographic Imager (CASI) sensor of NERC was used as the standard for this study. This CASI-2 is owned and operated by NERC and is calibrated to radiance in a laboratory procedure defined by Itres (Rollin *et al.* 2002). It is known to be a stable and accurately calibrated instrument,

comparable with laboratory calibration (Rollin *et al*. 2002; Choi *et al.* 2004; Riedmann, 2003). The graph (Figure 4-5) gives an indication of the NERC-CASI (CASI-2) calibration quality from an experiment described by Rollin *et al*. (2002).

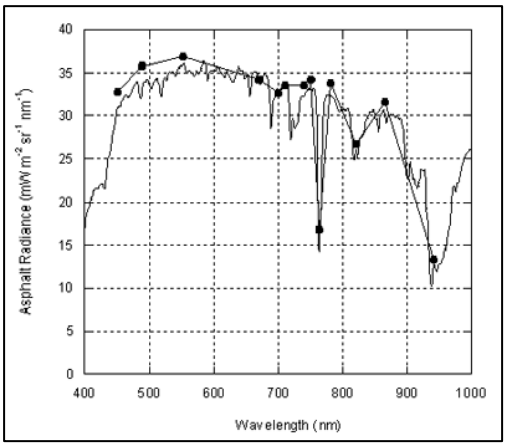

Figure 4-5 Comparison between the spectral radiance of an asphalt ground calibration target (continuous line) and CASI-2 data collected from an altitude of 853 m above sea level (dots). (Rollin *et al.*2002)

The ground targets to be used and the region-of-interest (ROI) for the study was identified in the fifth flight line for both the Eagle and CASI-2 sensor. NERC-ARSF delivers data in Level-1b (Appendix-E Data Level). This required the data to be corrected to Level-3a and exported in an image format (GeoTIFF used in this case) using AZGCORR and AZEXHDF software as used by NERC. The nomenclature of the file included the initial of sensor, Julian day, flight line number and data level. (Eg: e168051b). The command lines used for the correction, and converting to image format are as below, details of which are explained in the Appendix-F.

```
Eagle:
```
- `azgcorr -v -in -l 5513 6277 -cspacM -mUK99 osgb02.txt -be -p 1.0 1.0 -1 e168051b.hdf -3 e16805sub3a.hdf -eh chilbolton_5m.dem`
- `azexhdf –h e16805sset3a.hdf –G e16805sset3a.tif`

```
CASI:
```
- `azgcorr -v -be -l 4202 4729 -p 2.0 2.0 -1 c168051b.hdf -3a c16805sset3a.hdf -mUK99 osgb02.txt -eh chilbolton_5m.dem`
- `azexhdf –h e16805sset3a.hdf –G e16805sset3a.tif`

The Level-3a GeoTIFF image was imported in ENVI environment and an ENVI compatible BSQ format was created (a prerequisite format for subsequent

atmospheric correction in ATCOR 4 environment). The GeoTIFF image was created as an intermediate format instead of directly exporting to BSQ format since it was observed to retain the geometric fidelity of the image accurately. Spatial and spectral resampling was performed on both CASI-2 and Eagle respectively in order for them to be comparable with each other. The 2m spatial resolution CASI-2 data was spatially resampled to that of 1m of Eagle, which helped in identifying and delineating the targets. The 244 band Eagle data was spectrally resampled to that of 15 bands of CASI-2 in order to match with the wavelengths and the FWHM. The spectral resampling method opted in ENVI used both the wavelength and the FWHM information. The bottom up approach of resampling in the spectral domain was made in consistent with, towards arriving at the 3-bands of the SPOT-HRG bandwidth. Four homogenous patches based on visual estimation were identified comprising of (i) asphalt, (ii) fallow land (iii) grass type-1 and (iv) grass type-2. Random samples were generated from within each of the four homogenous patches totalling to 995 pixels. The samples were assumed to be normally distributed as they were extracted from within a single land cover type. (Appendix-G: four ROIs).

Evaluation of the Eagle sensor was based on relative measurements, comparing with the CASI-2 sensor taken to be the standard. The CASI-2 is assumed to be accurately calibrated with a linear radiometric response based on literature review (Rollin *et al*. 2002; Choi *et al*. 2004; Riedmann, 2003; Milton et al., 2004) and no test were carried out on CASI-2 to corroborate the same. The principle was, if measured radiance were same or similar between the two instruments, it would indicate similar calibration quality and the dispersion of the measured radiance between the two sensors in a scatter plot along with the coefficient of determination (R^2) would indicate the similarity in radiometric response between the two. Assuming CASI-2 to be linear, therefore a high degree of similarity would indicate a linear radiometric response for the Eagle sensor and vice versa.

An independent sample t-test with ($\alpha = 0.05$) was performed to find out statistically whether radiance measured under identical operational condition by Eagle is significantly different to that of CASI-2. The radiometric linearity of the Eagle was then checked by plotting the radiance from those 995 samples each from the Eagle and the CASI-2 data in the scatter plots. A ‘fit line’ was then added and the coefficient of determination (R^2) was calculated. Figure 4-2 illustrates the process flow-I.

4.2. Description of Process Flow -II

Creating an accurate reflectance map from the Eagle data involved a few intermediate steps and demanded some basic understanding of radiative transfer and role of ground targets. A brief note on the use of ATCOR-4's handling and some tips and tricks acquired in the process is mentioned in the Appendix-H for the interested. The atmospheric correction procedure adopted was of a hybrid nature called RTGC (USGS) proposed by Roger Clark developed at the USGS. At first three control files were created for the AISA-Eagle sensor – the calibration, wavelength and sensor definition files as described in Table 4-1 below:

Table 4-1 Control files for ATCOR 4

Control file	Purpose
arsf_eagle.cal	contained the gain and offset required to convert DN to radiance.
arsf_eagle.wvl	consisted of three columns (i) band no (ii) wave centre (wvc) µm and (iii) Full Width at Half Maximum (FWHM) µm.
arsf_eagle.dat	FOV in decimal degrees, number of pixels per line, band numbers, tilt and gain which were set at zero.

'Scan angle file' was created within the ATCOR 4 environment using the (i) header information of the image file, (ii) the flying altitude and (iii) the FOV of the sensor. 'Response files' were then generated for each band of the charged couple device (CCD) array. The response filters at such narrow FWHM of wavelengths, were treated as rectangular. ATCOR4 uses a high resolution (monochromatic) atmospheric Look-Up-Table (LUT), created using MODTRAN-4 Radiative Transfer code. A function called 'RESLUT' allows this LUT to be resampled into desired aerosol type at a defined altitude. 'Flight and Solar Geometry' were calculated with inputs taken from the flight metadata using an utility called HDF Explorer. The parameters used in ATCOR 4 are described in Table 4-2 below:

Table 4-2 Description of parameters used in ATCOR 4

Inputs	Parameters	Derived from
Date and time of data acquisition	17-06-2006; 11:54:04 (UTC)	Flight metadata
Geographic coordinate (dd)	Geo.Lon (-1.4); Geo.Lat (51.1)	Flight metadata
Flight altitude (km)	1.62	Flight metadata
Ground elevation (km)	0.88	Ancillary and field report
Flight heading (dd)	148˚	Flight metadata

Inputs	Parameters	Derived from
Solar Zenith Angle	29.4˚	Calculated viz. ATCOR with inputs from metadata
Solar azimuth angle	155.5˚	Calculated viz. ATCOR with inputs from metadata
Aerosol type	Rural	Ancillary and field report
Atmospheric water vapour column [cm]	2	NASA calibrated Aeronet Cimel data
Measurement of ground calibration targets	Reflectance spectra in the reflective solar zone	Field measurements

Once all the control files, derived parameters and requisite information had been generated and converted into the required units, the 'atmospheric correction for flat terrain' option in ATCOR was launched. The rationale of selecting 'flat terrain' was because of the generally flat topography and the small study area. A scale factor of 100 was used in order to store the 4 byte output float data as a 2 byte integer, reducing the file size to half with no significant loss of information, a consideration saving when dealing with hyperspectral datasets (Richter, 2008). After selecting the appropriate atmospheric file which contained the correct altitude, water vapour column and aerosol type, the ATCOR 'SPECTRA' module was used to update the sensor calibration file based on measured ground spectra. Radiometric calibration assumes nominal sensor parameters (Richter, 2008), so spectral calibration must precede any recalibration of radiometric calibration coefficient. Ground calibration targets of contrasting albedo (concrete and asphalt) were used in the process and a new spectral calibration file was generated with spectral shifts per spectrometer with a new centre wavelength for all channels. Measured atmospheric parameters and ground reflectance were then used to calculate the new coefficients C_0 and C_1 (offset and slope) for each band and the new radiometric calibration was computed. Appendix I shows the results from the spectral and radiometric calibration. Finally the 'Image Processing' option in ATCOR 4 was used to create a standardised and corrected reflectance map from the Eagle hyperspectral data shown in Appendix J.

Validation of the retrieved surface reflectance map was then carried out by both direct and indirect methods to gain confidence in the derived dataset. Direct validation was carried out by using the grey and black ground targets. Indirect validation was carried out by comparing with an independent reflectance map generated from an independent CASI-3 sensor flown by Environment Agency about an hour prior to the NERC CASI-2 at a much higher altitude. In order to be

comparable the 244 band Eagle reflectance map was then spectrally resampled to the 32 spectral bands of EA-CASI (CASI-3) based on wavelengths and FWHM.

The comparison and validation were carried out by calculating the "Absolute Difference" and "Relative Difference" in reflectance for bands which when aggregated make up for each band of SPOT-HRG. While aggregating the individual bands of Eagle and CASI-3 to match with that of SPOT, equal weights were given to each bands. The mean, standard deviation, standard error and confidence interval at a level of significance ($\alpha = 0.05$) were calculated and compared between ground spectra (grey and black target) and Eagle reflectance map and between EA-CASI-3 reflectance map and the Eagle reflectance map. With the artificial target validation, all the available field measurements were used. For validation with the EA-CASI, random pixels from each land cover class of grass, asphalt and concrete were taken. Figure 4-3 illustrates the process flow-II.

4.3. Description of Process Flow -III

The SPOT-HRG data was spectrally subset to contain the solar reflective region and a spatial subset of cloud free area of approximately 225 sq km as shown in the Figure 4-6 below. Three calibration targets (asphalt, grass and bare soil) could be identified from the Eagle reflectance map which best matches the requirements as laid down in the literature review section. Mean reflectance spectra from each target were calculated and were resampled to that of SPOT wavelengths. These three mean spectra would form the three point regression equation of the ELM model. Calibration spectra from the SPOT image were also collected and the ELM was performed in ENVI to derive a reflectance-calibrated map. The map was then validated with the Eagle reflectance map and then compared to an independent reflectance map derived from the same SPOT data which was atmospherically corrected using a direct radiative transfer method employing ATCOR 2 software. To validate with the Eagle reflectance map required the Eagle map to be spectrally and spatially resampled to the three SPOT-HRG bandwidth with 10m pixel resolution. Absolute and Relative difference in reflectance was then calculated in a process similar to as discussed in process flow-II except no band aggregation to match up with SPOT-HRG was required at this stage. Comparison was made between the Eagle map and ELM corrected SPOT image and between Eagle map with ATCOR 2 corrected SPOT image. Figure 4-4 illustrates the process flow-III.

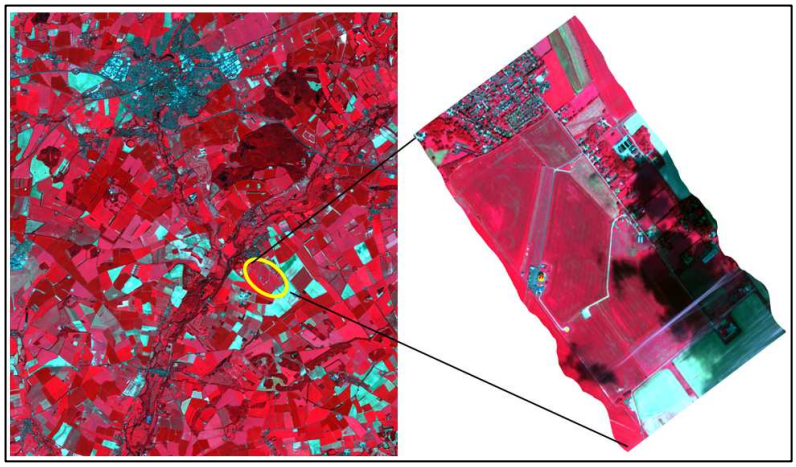

Figure 4-6 The left part shows the SPOT subset and the right part the Eagle subset of the study area.

5. Results and Discussions

5.1. Results and discussion for the AISA-Eagle evaluation

The calibration quality and linearity of the Eagle sensor was compared against the CASI-2 sensor which was taken to be the standard for this study. It was assumed to be a stable, accurately calibrated and linearly designed sensor based on literature review (Choi *et al*. 2004; Riedmann, 2003).

Results:

Calibration quality of Eagle was evaluated using a series of two-tailed independent sample Student t-test. This statistical procedure tested the significance of difference between the means of measured radiance by the Eagle and the CASI-2 sensor for each wavelength at a significance level of ($\alpha = 0.05$). The null hypothesis (H_0) and the alternate hypothesis (H_a) therefore were stated as:

H_0: $E_{L(\lambda)} - C_{L(\lambda)} = 0$

H_a: $E_{L(\lambda)} - C_{L(\lambda)} \neq 0$ $\alpha = 0.05$

where, $L(\lambda)$ = radiance (L) measured for wavelength (λ) ; E= Eagle; C=CASI-2 and α = level of significance. Sample size were equal (n) =995 and the two distributions were assumed to be normal. The null hypothesis states that mean of measured radiance under identical operational condition by Eagle and CASI-2 is equal. The t-test showed a very low p-value ($p = <0.001$) for each wavelength allowing to reject the null hypothesis and accept the alternate (Appendix-K. t-test result). At 95% confidence level it can be said with certainty that the measured radiance of Eagle was significantly different with that of CASI-2. This test concludes a poor calibration of Eagle at its present form compared with that of CASI-2 sensor (Research Question-1). Figure 5-1 and Table 5-1 shows the concised result.

The radiometric response of the Eagle sensor was checked by plotting the measured radiance of the 995 sample, from both the sensors in the scatter plots. A fit line was added to each plot and the coefficient of determination (R^2) was calculated (Figure 5-2). The selected wavelengths to represent the SPOT bands were 0.5535 μm, 0.6524 μm and 0.8221 μm and the calculated R^2 values were 0.955, 0.98 and 0.986 respectively. The dispersion of scatter plots together with the R^2 values, suggested a highly similar response with CASI-2, allowing to deduce a linear radiometric response for the Eagle sensor compared with the CASI-2 (Research Question 2).

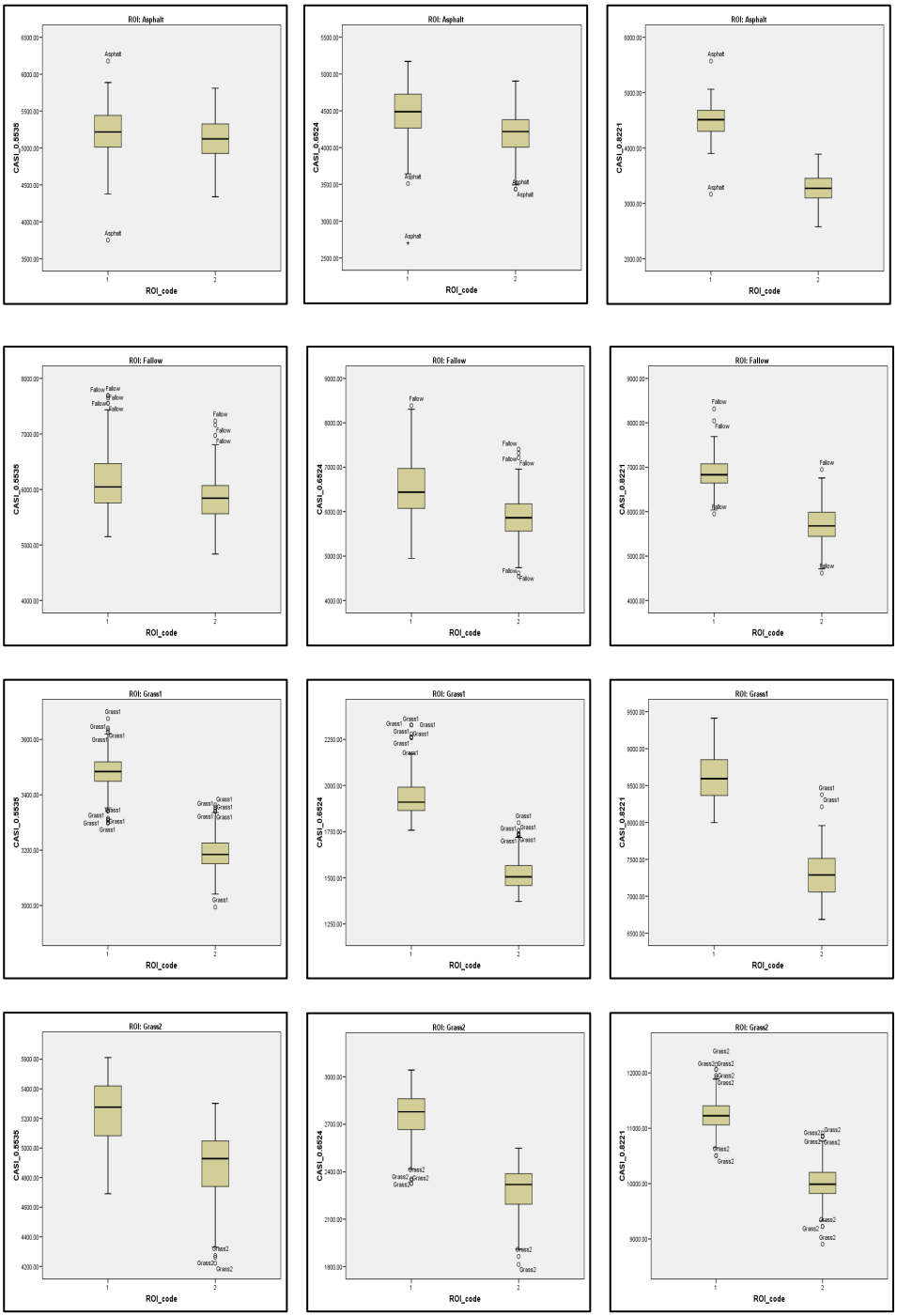

Figure 5-1 Box-plot showing radiance measured by both sensors is significantly different in each SPOT-comparable bands for the four ROIs.

Table 5-1 t-test of measured radiance between CASI-2 and Eagle at p=0.05

Wavelengths (micrometers)	p-value (2 tailed)	Significantly different between CASI-2 and Eagle sensor
0.4512	p < 0.001	Yes
0.4914	p < 0.001	Yes
0.5535	p < 0.001	Yes
0.6095	p < 0.001	Yes
0.6524	p < 0.001	Yes
0.6724	p < 0.001	Yes
0.7031	p < 0.001	Yes
0.7126	p < 0.001	Yes
0.7433	p < 0.001	Yes
0.752	p < 0.001	Yes
0.7645	p < 0.001	Yes
0.7828	p < 0.001	Yes
0.8221	p < 0.001	Yes
0.8664	p < 0.001	Yes
0.9413	p < 0.001	Yes

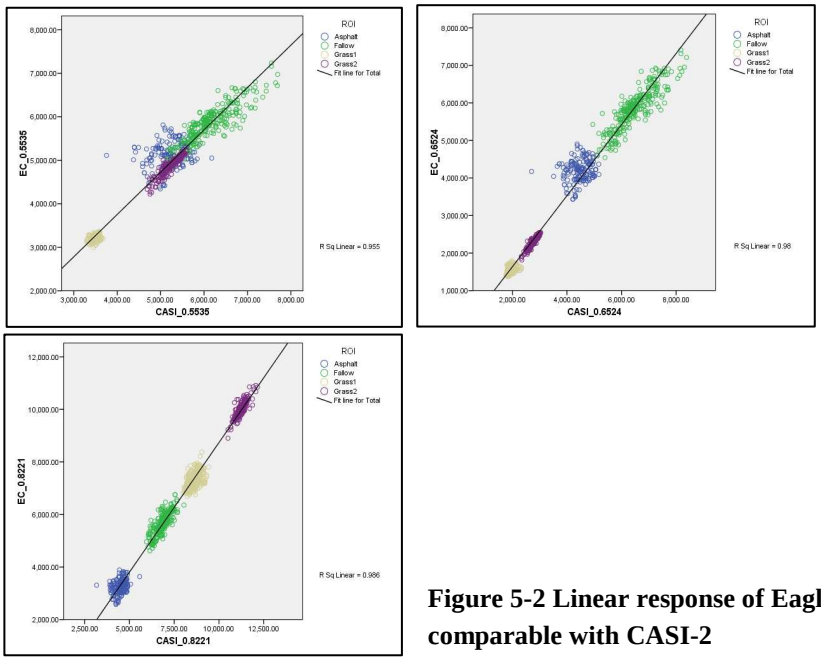

Figure 5-2 Linear response of Eagle comparable with CASI-2

Discussion:

The paradigm of Cal-Val depends on relative measurements where absolute calibration of instrument is not essential provided it is stable and has a linear response (Milton *et al*. 2007, Gao *et al*. 2006). Most sensors are designed to be linear, where digital output *X* being proportional to the radiance *L (X=AL)* after dark signal subtraction. To account for non-linearity of sensor, a polynomial equation can be adopted $(X=AL + BL^2)$. Calibration method provide the absolute calibration coefficient *A* and if necessary *B* (Dinguirard and Slater, 1999). Relative calibration is achieved by normalising the output of different sensor so that they all give the same value when viewing a stable, spatially uniform radiance field (Milton, 2004).

In this study, first the calibration of Eagle was evaluated by comparing the radiance measured from same features by both sensors under identical operational condition. It was a rare opportunity where both the sensors, CASI-2 and Eagle were mounted on the same aircraft and imaged simultaneously ensuring identical atmospheric condition, illumination, roll, pitch, yaw of aircraft, solar zenith angle, azimuth angle etc. The calibration error of the Eagle sensor do not mean that it cannot be used as a transfer standard, it merely indicates that one should not rely on the radiance value it measures, and therefore it is unsuitable for any 'radiance method' (Dinguirard and Slater, 1999) This also points out to the need of calibration for the Eagle sensor.

Linearity of a sensor can be explained when a linear function express uniform gain and coefficient for a detector. This means same features may get measured at different value ranges by different sensors as a function of their calibration accuracy but may exhibit similar trend in radiometric response between sensor DN and radiance. As described by Dinguirard and Slater (1999) it can be inferred that in its present calibration form, the Eagle data cannot be used for any radiance-based method but may effectively be used for any reflectance-based method provided the radiometric response of the instrument is linear which was so found.

5.2. Results and discussion of the Eagle reflectance map.

The Eagle reflectance map was prepared using the RTGC (USGS) method and was validated applying both direct and indirect method, using the field measured grey and black artificial targets and by an independent reflectance map generated from EA-CASI (CASI-3) sensor flown by the Environment Agency (EA) on the same day. Results were compared and expressed for the bands which when aggregated match the three SPOT wavebands. Absolute and relative difference was calculated between the modelled and the observed reflectance. Since reflectance is measured in percent, the relative difference was in actuality the percent of the percent.

Identifying suitable ground calibration targets from the reflectance map for applying ELM to correct the SPOT-HRG is also discussed here.

Results:

Direct validation (Figure 5-3a; Table 5-2 to Table 5-3) with grey target showed good result with absolute reflectance difference of within ±1.6 for band-2 and band-3 and -2.4 in SPOT comparable band-1. With black target, the absolute difference was less than 2 for band-1 and band-2 but a high value of 3.87 in band-3. Inspection with the asphalt and concrete targets showed excellent similarity between the field spectra and the Eagle data, however, this was to be expected as these sites were used in generating the reflectance map, so this was not a fair validation and indirect validation was carried out.

Indirect validation of the reflectance map proceeded using data from an independent CASI-3 system flown by the EA agency. Figure 5-3b shows the result for grass, asphalt and concrete with absolute difference ranging between -0.97 to 1.52 (Table 5-4 to Table 5-6; where 'E-C' represents Eagle bands resampled to CASI-3 bands). No clear or significant difference was observed. The means were similar and the 95% confidence interval on those means overlap (Appendix-L: Confidence Interval on Validation). It is hence concluded that the Eagle reflectance map is sufficiently accurate to be used for up-scaling to SPOT-HRG data (Research Question 3).

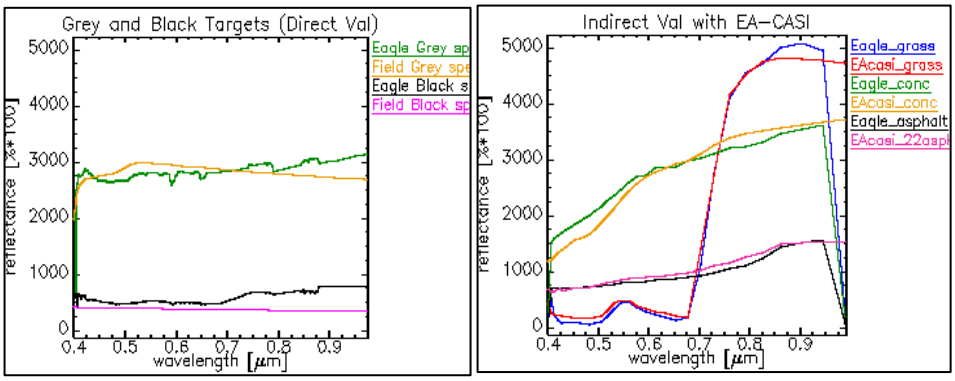

Figure 5-3 Comparison with (a) grey and black targets (b) with EA-CASI map

The reflectance map was studied carefully and three ground calibration sites of varying albedo were identified (grass asphalt and concrete) to be used in the ELM model to correct the SPOT-HRG. In doing so, care was taken to select targets that fulfilled the requirements set out in the literature reviewed in Chapter 2, especially in respect of (i) size of target, (ii) range of reflectance and (iii) stability over time.

Considering the size in relation to SPOT pixels, identifying grass as a calibration target was no problem, bare soil representing bright albedo could also be delineated with some difficulty. It was more difficult to find a large dark target, however the area of asphalt was accepted as the best available within the immediate area.

Considering range of reflectance in each band, only three targets (asphalt, grass and bare-soil) could be identified within the constrained study area. The reflectance of these three targets essentially brackets the boundary of the mixing space within which objects of interest were to be found. Typically, more the mixing space bounded by pure spectra, better the ELM would perform. With only asphalt representing the dark and bare soil representing the bright area, the range of reflectance in each band was compromised to within a limited mixing space. Furthermore, Lambertian assumption is less realistic for bare soil and directional effect and heterogeneity of the soil complicates the matter.

In terms of stable composition over time, i.e. without shadow, water or sun glint etc, features could be identified with sufficient ease. Some regions in the east and south-eastern part had to be avoided due to cloud cover.

Therefore it can be concluded that although it was challenging to find desirable targets within such a small study area, nevertheless the Eagle reflectance map can be used to identify suitable calibration targets for ELM (Research Question 4). The main constraint of finding more number of suitable ground calibration targets with varying albedo, that could form the many regression points during ELM calibration was compromised primarily by the limited extent of the study area. (Figure 5-4 shows the three ground calibration targets)

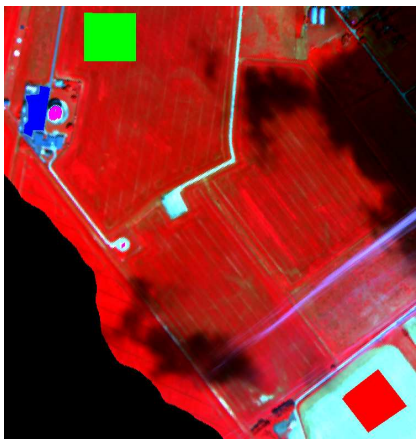

Figure 5-4 Three suitable ground calibration targets identified for SPOT-HRG ELM. (Green is grass, blue is asphalt and red is bare soil)

Table 5-2 Direct validation with grey target

SPOT Bands	Eagle bands	Absolute difference	Relative Difference%
1	E(47-83)	-2.42	-8.03 %
2	E(95-121)	-1.63	-5.54 %
3	E(166-208)	1.34	4.78 %

Table 5-3 Direct validation with black target

SPOT Bands	Eagle bands	Absolute difference	Relative Difference%
1	E(47-83)	1.76	53.47 %
2	E(95-121)	1.63	51.46 %
3	E(166-208)	3.87	129.82 %

Table 5-4 Indirect validation with 20 random grass samples

SPOT Bands	Eaglew.r.t.EACASI	Absolute difference	Relative Difference%
1	E-C(15-19)	-0.54	-12.95 %
2	E-C(21-24)	-0.97	-19.56 %
3	E-C(28-30)	1.52	3.18 %

Table 5-5 Indirect validation with 22 random asphalt samples

SPOT Bands	Eaglew.r.t.EACASI	Absolute difference	Relative Difference%
1	E-C(15-19)	-0.62	-7.33 %
2	E-C(21-24)	1.43	15.00 %
3	E-C(28-30)	-0.51	-3.57 %

Table 5-6 Indirect validation with 21 random concrete samples

SPOT Bands	Eaglew.r.t.EACASI	Absolute difference	Relative Difference%
1	E-C(15-19)	1.46	6.09 %
2	E-C(21-24)	-0.29	-0.98 %
3	E-C(28-30)	-1.31	-3.7 %

Discussion:

In a strict sense the direct validation of Eagle reflectance with respect to ground targets could only be made with the grey target. A black target is not suitable for such calibration practices. A true black target should give zero reflectance with only the path radiance registered as the ‘at-sensor-radiance’ which is too idealistic to be true in any operational condition. The presence of a ‘red edge’ in the average Eagle spectrum from the black target shows that it was contaminated by the grass

background, either because it was too small to completely fill the field-of-view or because the adjacency effect was not accurately modelled by the ATCOR program. This result was not unexpected as the artificial targets were only 6m x 6m in size, and of necessity were placed on a healthy green vegetation background, so retrieving the accurate reflectance for the black target in particular was always going to be a challenge and hence the high difference in absolute value for band-3. The very low numeric value as the denominator also explains the high value in band-3 while calculating for the relative difference of the black target. Also for dark targets, even a very small contamination of contrasting material could significantly change the reflectance (Smith and Milton, 1999). A visual inspection alone might not be sufficient to identify targets with enough spectral contrast (Price, 1994).

There is a need to understand the intrinsic nature and behaviour of the ground targets used during calibration and validation of this study. The white target could not be used for either calibration or validation because of the high gain of Eagle sensor left it saturated. Once a pixel gets saturated, subsequent values in the following wavelengths even if registered are unreliable. This is because the way the programme is written in the imaging software where the values registered in the lower wavelength is used to trigger the values in the next higher wavelengths. Therefore, once a pixel gets saturated all values along the subsequent bands for that pixel become unreliable (Llewellyn, pers. comm. Nov.2008). The concrete calibration target was found to be spectrally heterogeneous which could have introduced some artefacts in the reflectance map resulting in residual errors although asphalt seemed to be more stable spectrally and spatially.

One interesting finding was the pattern in which similar spectra were oriented. They lied roughly in a north-south direction i.e. along the flying direction. Discussion with Gary Llewellyn the Science Coordinator of NERC-ARSF revealed that due to the low flying altitude and the integration time of imaging frame per seconds (fps) used with the given Eagle-IFOV, the effective ground sampling resolution (GSD) of the pixel turned out to be an elongated rectangular shape in the raw data. Pre-processing of the raw data and resampling to 1 meter still retained the trait of the original GSD and its corresponding point spread function (PSF) as shown in Figure 5-5. This possibly explains the smearing effect of similar spectra in the direction of flying, spread roughly over three pixels. This also points out to the need of proper synchronisation of flying altitude with the imaging instrument in use to achieve an output data of desired quality.

Figure 5-5 Elongated spectra

The indirect validation was based on comparing similar products from independent sources; a method akin to how NASA evaluates MODIS with products such as AVHRR, SeaWiFS, MERIS, SPOT-VGT etc (Morisette *et al* 2002; http://landval. gsfc.nasa.gov/index.html). The principle is, if similar standardised product gives comparable results, it establish confidence in datasets. The EA-CASI was flown on the same day about an hour before at a much higher altitude than Eagle. The reflectance map generated from it also used the same RTGC (USGS) correction method using the grey and black ground targets. Results showed a close match between the two products with no clear or significant differences. The means are similar and the 95% confidence intervals on those mean overlap (Appendix I). This reasonably builds confidence in the Eagle reflectance map. For grass, asphalt and concrete the absolute differences lied within a nominal -0.97 to 1.52.

It is however to be borne in mind that an exact match is not feasible nor to be expected between the field and scene spectra. Field measurements can have inherent uncertainties which can be significant, owing to factors such as Hemispherical Conical Reflectance Function (HCRF), instability of instrument, uncertainty of standards used to calibrate these instruments, principles and techniques used for reducing measurement errors and likewise. There are also issues with respect to spatial distribution of field measurements and the number of readings. The variability in field measured reflectance factors for non-Lambertian surface are contributed by varying solar zenith and other atmospheric conditions (Milton *et al.* 2007). Metadata of field measurements of the targets during the NCAVEO campaign showed they were not exhaustive. It ranged from measurements taken at point location (eg. concrete) to a small subset region (eg. 3m x 3m for asphalt) and therefore not necessarily always represented the whole target feature, specially for the spectrally unstable. Validations with the ground targets were carried out between the scene spectra and the target feature, and were not aligned to match with the exact

coordinates from where the readings were taken. Because of all these practical considerations there will always be some deviation from the observed.

In most cases it may be expected that there will always be some practical constraints in terms of field measurements and characterisation of targets. More important is the awareness of such uncertainties which needs to be documented in order to estimate whether the difference between observed and predicted explains the situation and if gives plausible results thus imparting confidence in data and to have traceability. Ideally speaking, the spatially large, near-Lambertian surface without micro-relief, spectrally stable and bland targets are to be best found only in desert surface, river bed playa and alkali flats such as used in in-flight vicarious calibration sites in deserts of Nevada or White Sands in New Mexico or similar. Achieving accurate and precise atmospheric correction is not an easy task which requires careful planning and examination of flight data and comparison of field data. Clark in 2002 noted that even with high signal to noise ratio of AVIRIS data it typically requires 1 to 2 person months per study site to achieve a quality calibration. Eagle data can generate accurate reflectance map and can be used in any reflectance based method. More detailed conclusion about sensor and data quality would require more detailed and formal calibration and validation.

5.3. Result and discussion of the ELM on SPOT-HRG

The SPOT–HRG was atmospherically corrected using ELM method applying the three ground targets identified from the Eagle reflectance map. The SPOT data is then validated with the Eagle reflectance map and also with an independently corrected map of the same SPOT data which used RT method employing ATCOR 2.

Result:

The ELM corrected SPOT-HRG data was in close match with the Eagle reflectance map. Comparing the three bands, with asphalt, grass (near nadir) and grass (off-nadir) the absolute difference between Eagle and ELM corrected SPOT ranged between (-1.06 to 1.50), (-0.72 to 0.36) and (-0.93 to -0.51) respectively; compared to the high difference between Eagle and ATCOR-2 corrected SPOT of (2.59 to 6.03), (2.51 to 10.80), and (2.28 to 11.10) respectively. However for bright targets such as bare soil and bright vegetation, the ELM did not showed marked improvement over ATCOR-2 corrected and was comparable. Figure 5-6 and Table 5-7 to Table 5-11 show the graph plots with the results and Appendix L show the 95% confidence interval on the means. It is therefore concluded that Eagle reflectance map can be used to atmospherically correct SPOT-HRG to provide a validated and calibrated data product (Research Question 5).

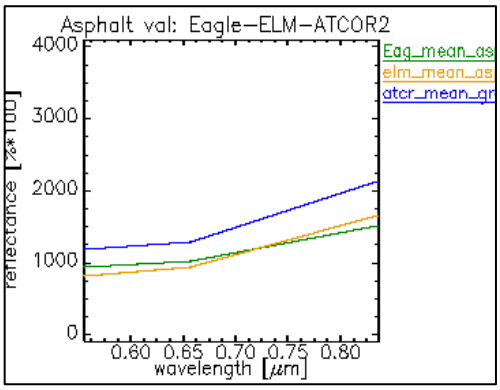

Fig. 5-6 (a)

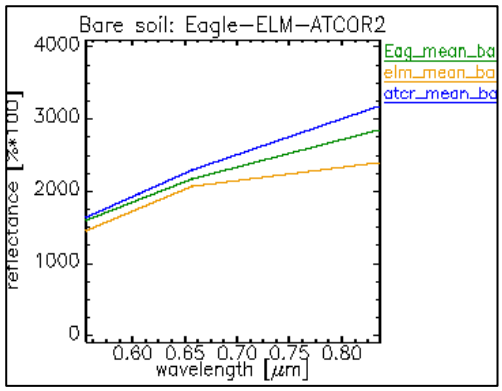

Fig. 5-6 (b)

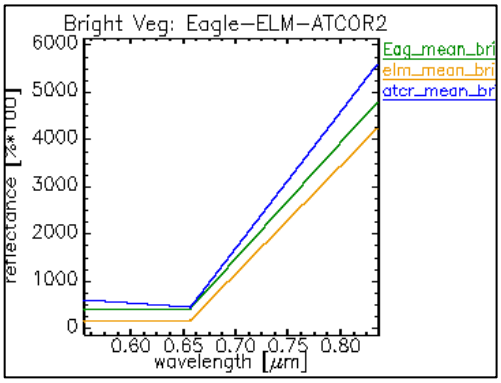

Fig. 5-6 (c)

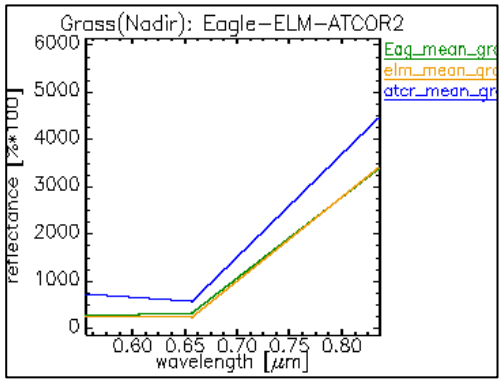

Fig. 5-6 (d)

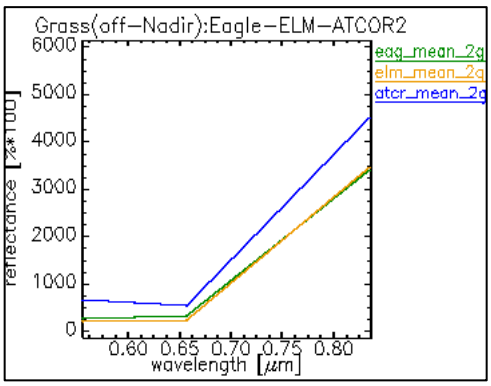

Fig. 5-6 (e)

Figure 5-6 (a) Asphalt, (b) Bare soil, (c) Bright vegetation, (d) Grass (near-nadir) and (e) Grass (off-nadir)

Table 5-7 Validation with asphalt

SPOT bands	Eagle Vs SPOT – ELM		Eagle Vs SPOT – ATCOR	
	Absolute diff	Relative diff	Absolute diff	Relative diff
Band1	-1.06	-11.54	2.63	28.59
Band2	-0.75	-7.47	2.59	25.71
Band3	1.50	9.86	6.03	39.4

Table 5-8 Validation with bare soil

SPOT bands	Eagle Vs SPOT – ELM		Eagle Vs SPOT – ATCOR	
	Absolute diff	Relative diff	Absolute diff	Relative diff
Band1	-1.38	-8.77	0.50	3.20
Band2	-0.91	-4.24	1.40	6.51
Band3	-4.63	-16.17	3.2	11.44

Table 5-9 Validation with bright vegetation

SPOT bands	Eagle Vs SPOT – ELM		Eagle Vs SPOT – ATCOR	
	Absolute diff	Relative diff	Absolute diff	Relative diff
Band1	-2.19	-59.89	2.41	65.75
Band2	-2.46	-62.23	0.51	13.05
Band3	-5.83	-12.02	7.90	16.29

Table 5-10 Validation with grass (off-nadir)

SPOT bands	Eagle Vs SPOT – ELM		Eagle Vs SPOT – ATCOR	
	Absolute diff	Relative diff	Absolute diff	Relative diff
Band1	-0.08	-3.32	4.47	169.70
Band2	-0.72	-23.39	2.51	81.38
Band3	0.36	1.08	10.80	31.78

Table 5-11 Validation with grass (near-nadir)

SPOT bands	Eagle Vs SPOT – ELM		Eagle Vs SPOT – ATCOR	
	Absolute diff	Relative diff	Absolute diff	Relative diff
Band1	-0.57	-21.48	4.05	151.68
Band2	-0.93	-30.39	2.28	73.86
Band3	-0.51	1.49	11.10	32.28

Discussion:

The SPOT image was acquired on 10th June, 2006 a week before the 17th June, 2006 when most of the multiple concurrent RS and field data were acquired. This one week time lag could be overlooked for performing the ELM provided the targets remained spectrally stable over that period of time (Teillet *et al*. 1990; Karpouzli and Malthus, 2003). Meteorological data and ancillary information suggested a stable atmospheric condition over that week to have any significant contribution on the target stability. The ELM performed on the SPOT-HRG data used only three regression points, which can be rightly argued by experts to be insufficiently low. The very small region-of-interest taken for the study left with this constraint of not finding in enough numbers, suitably large homogenous targets of varying albedo to be used as ground calibration targets. Although on the other hand it offered a unique opportunity to compare between two corrected datasets - a rudimentary ELM using only three regression points taken from the validated Eagle reflectance map against a directly atmospheric corrected map which used robust RT based code employing ATCOR 2.

An agreeable and plausible result which matched closely with the Eagle reflectance was achieved by the ELM except for very bright features. The reason is best believed to be of insufficient characterisation of bright target as ground calibration, considering range of reflectance in each band. The mixing space allowed by the bare soil as the threshold for the bright reflectance range was insufficient to accommodate the very bright features. As sufficiently large similar bright targets could not be identified in the Eagle reflectance map, this lead to the relatively poor correction for the very bright features. For other features that were checked, the transfer standard based ELM corrected SPOT data was found to be more accurate than ATCOR corrected SPOT manyfold. The reason for the poor match of bright targets was traced back to the constraint laid by the limited extent of the study area. From the result, it is however reasonable to deduce, that given a large study area, identifying suitable and in sufficient numbers of ground targets would be easier to form the many regression points required to perform a good ELM. The then corrected result would be far more accurate for all features in each band than other conventional direct method of atmospheric correction which do not use any transfer function. This transfer standard method of atmospheric correction of SPOT HRG offers the users to use the validated data with more confidence than compared with others. The user is now aware of where and for which features there lies a potential possible source of error. It also allows for the error to be traced back all the way to the transfer standard and even to the ground. This allows for allowances and adjustments while working with such validated data. This is one of the primary goals

of “cal-val” which aims to provide data with known standard of quality. Atmospheric correction of SPOT–HTG using a transfer standard gave more plausible result than the only RT corrected method except for very bright features. The study concludes that Eagle reflectance map can be used to atmospherically correct SPOT-HRG in providing a validated and calibrated data product.

5.4. Assumptions and Limitations in the Methodology

1. No test of normality was performed for the four ROIs from where 995 samples were taken assuming it to be normal since picked from same landcover type.
2. The most accurate method of spectral resampling would be based on the known SRF of the sensor. In absence of that, as in this case, the next best available option was chosen which uses the band-centre and the FWHM.
3. At such narrow FWHM of the Eagle, the spectral response was assumed to be rectangular and hence rectangular filters were generated for the same.
4. Calculating solar geometry requires accurate time and scene centre coordinates. Flight metadata provides the time and the extent of the coordinates for particular flight line. The time and scene centre was therefore estimated for the subset of the fifth flight line which was taken to be the study area. This was inevitable but nevertheless affected with the HCRF effect. Effect of such angular resolution could be significant in determining the quality of atmospheric correction specially for albedo estimation.
5. The exact altitude of the aircraft over the study area was assumed to be the average flying height while calculating the AOT at that altitude.
6. Owing to the limited study area, it was challenging to find suitable ground calibration targets and the numbers of calibration targets used were the bare minimum to form the ELM regression. This compromised with attaining a very good ELM.
7. For calculating the results of the absolute and relative difference for reflectance, the number of Eagle and CASI bands which aggregate to match the SPOT wavebands were given equal weightage which assumes the SRF of SPOT to be rectangular in order to fit. At such broadband such as SPOT, it is expected to be gaussian and hence a weighted average would have been more appropriate.
8. Indirect validation data (the EA-CASI reflectance and the ATCOR-2 corrected SPOT reflectance map) was assumed to be correct.

6. Conclusions and Recommendations

6.1. Summary

Potential of the Specim AISA-Eagle imaging spectrometer as a transfer standard for atmospheric correction of SPOT-HRG has been successfully established in this research. The Eagle sensor is also evaluated in terms of instrument calibration and linearity with that of CASI-2 sensor of UK NERC. The result expects to be of great practical importance to the users of NERC-ARSF facility who wish to use the Eagle data. The research demonstrated the requirement of a large study area for accurate atmospheric correction of high resolution satellite data such as SPOT-HRG using ELM coupled with a transfer standard mechanism. The has research also streamlined an effective and flexible process flow which could be transferred to similar scientific and operational applications involving imaging spectrometers to atmospherically correct high resolution satellite data. It is a value addition for such scientific application in the field of calibration and validation and contributes towards the larger realisation of offering validated EO products.

6.2. Conclusions with respect to the Research Questions

1. Addressing to the first research question, the calibration quality of the Specim AISA Eagle imaging spectrometer compared to that of the CASI-2 sensor of the NERC-ARSF was found to be of poor quality at its present form.
2. Addressing to the second research question, the radiometric response of the Eagle sensor was found to be similar with that of the CASI-2 sensor of the NERC-ARSF. Considering CASI-2 to be a linear sensor, the radiometric response of the Eagle imaging spectrometer was deduced to be linear.
3. Addressing to the third research question, it is concluded that the Eagle data can produce an accurate reflectance map for use in upscaling to SPOT-HRG.
4. Addressing to the fourth research question, it is concluded that the Eagle reflectance map can be used to identify suitable ground calibration targets for SPOT considering (i) size in relation to SPOT pixels, (ii) range of reflectance in each band and (iii) stable composition. A large study area representative of the surrounding landcover would facilitate finding with many suitable targets and also reasonably allow the assumptions associated with the ELM method.

5. Addressing to the fifth research question, it is concluded that the Eagle reflectance map can be used as a transfer function to atmospherically correct SPOT-HRG to provide a validated and calibrated data product.

6.3. Conclusions from the the Research as a whole

1. The Eagle imaging spectrometer can be effectively and efficiently used as a potential transfer standard for atmospheric correction of SPOT HRG data. The research demonstrated a simple and flexible process flow for atmospheric correction of high resolution satellite data in a scaled down framework of Eagle sensor and SPOT-HRG. With reasonable confidence it may also be inferred that the same technology can be transferred to similar civil EO satellites and imaging spectrometers.
2. In its present calibration form, the Eagle data is unsuitable for any radiance based method. However the data can be used with confidence for any reflectance based method.
3. Validation result of SPOT data suggested that even a rudimentary model, when coupled with a robust transfer standard can offer plausible atmospheric correction. .
4. The role of sensors of varying resolution for both aircrafts and space borne satellites lies not only in mapping at different scales, but are and can be used as an excellent transfer standards in upscaling and data aggregation for data of different resolution.

6.4. Limitations in the Research

1. There is scope for detailed in-depth investigation and research in each of the three major sub-groups viz. (i) evaluation of Eagle sensor (b) creating accurate reflectance map and (c) the ELM correction of SPOT-HRG using the Eagle reflectance map. The limited time constraint left further investigation within each sub-group beyond the scope of this research.
2. There is scope for more exhaustive quantitative analysis with respect to sensor evaluation, quality, traceability and uncertainty of the data product.
3. The NERC-CASI-2 sensor was assumed to be accurate in terms of calibration and linearity of the instrument and no test was performed to check that.
4. The measurements from field were also assumed to be accurate.
5. More formal and robust statistical validation is required to brand a product of its data quality.
6. The result of such a robust and accurate Eagle reflectance map was somewhat diluted using a very simple model such as the ELM to be used for atmospheric

correction of SPOT-HRG data. Additionally the limited ground calibration targets resulted in a weak ELM which could have been possibly avoided if a larger study area was taken in the first place.

7. Between field measurements on ground and the satellite data at TOA, this research primarily looked into the atmospheric effects, but there also lies the issue of spatial resolution looking into which remained beyond the scope of this study.

6.5. Recommendations

1. A laboratory calibration of Specim AISA-Eagle sensor is recommended. Because operational aircraft environment (temperature, humidity, vibrations etc) differs from that of laboratory, the sensor should then be checked at regular intervals by in-flight vicarious calibration in order to provide radiance calibrated data product.
2. Given the need of today and rising willingness within users, data providers and stakeholders, a detailed and comprehensive methodology could be formulated from this method under demonstration. Frequent flying with an imaging spectrometer can be accomplished over a large region preferably over instrumented sites to develop and compile the temporal variability of ground targets as Look-Up-Tables (LUT) in varying atmospheric conditions. These LUT can then be applied for atmospheric correction of high resolution satellite images traceable with known uncertainties for either the next stage of transfer function dealing with spatial resolution or directly as input to environment application or models.
3. Irrespective of whether the site is instrumented or not, an on-board atmospheric measurement unit in the aircraft can be a possibility. This would serve the dual purpose of proving accurate atmospheric data for correction at a later date and also would facilitate the operator to set the gain of the camera if required, based on the then present atmospheric condition of flying.
4. The sequence of process flow developed is flexible and could be replaced with more advanced or better available methodologies. For example, the ELM based method could be replaced with a more rigorous model.
5. The short note in the Appendix-H on the use of ATCOR-4 is aimed for the interested but inexperienced researchers.

6. Even within a scaled-down framework this research has attempted to look at the many facets of calibration and validation. There lies a unique opportunity for many advanced research which can sprout in many directions from this study. For example, a further investigation on calibration of Eagle sensor is possible, or generation of a more accurate reflectance map with detailed accounting of angular functions of HCRF, or developing a more robust model than ELM for atmospheric correction using the reflectance map or even further refinement and developing the whole process of evaluation and using imaging spectrometers as transfer standard. Further research is encouraged in this field for the advancement of the science and to achieve the “best practice” in the field of calibration and validation of sensors and data products.

REFERENCES

ADLER-GOLDEN, S. M., MATTHEW, M.W., BERNSTEIN, L.S., LEVINE, R.Y., BERK, A., RICHTSMEIER, S.C., ACHARYA, P.K., ANDERSON, G.P., FELDE, J.W., GARDNER, J.A., HOKE, M.L., JEONG, L.S., PUKALL, B., RATKOWSKI, A.J. AND BURKE, H.K. (1999) Atmospheric correction for shortwave spectral imagery based on MODTRAN 4 IN GREEN, R. O. (Ed.) *Eighth JPL Airborne Earth Science Workshop*. Pasadena, CA, JPL Publ. 99-17, Jet Propulsion Laboratory.

ANDERSON, K. & MILTON, E. J. (2006) On the temporal stability of ground calibration targets: implications for the reproducibility of remote sensing methodologies. *International Journal of Remote Sensing,* 27**,** 3365 - 3374.

BEN-DOR, E., KRUSE, F.A., LEFKOFF, A.B. & BANIN, A. (1994) Comparison of 3 calibration techniques for utilisation of GER 63-channel aircraft scanner data of Makhtesh-Ramon, Negev, Israel. *Photogrammetric Engineering and Remote Sensing,* 60**,** 1339-1354.

CARRERE, V. & ABRAMS, M.J. (1988) An assessment of AVIRIS data for hydrothermal alteration mapping in the Goldfield mining district, Nevada. IN VANE, G. (Ed.) *In Proceedings of the Airborne Visible/Infrared Imaging Spectrometer (AVIRIS) Performance Evaluation Workshop.* Pasadena, CA,, JPL Publ. 88-38 Jet Propulsion Laboratory.

CHOI, K. Y. & MILTON, E. J. (2004) Estimating the spectral response function of the CASI-2. *Annual Conference of the Remote Sensing and Photogrammetry Society*. Aberdeen, Scotland.

CLARK, R. N., SWAYZE, G.A., HEIDEBRECHT, K.B., GOETZ, A.F.H., & GREEN, R.O. (1993) Comparison of methods for calibrating AVIRIS data to ground reflectance. IN R.O.GREEN (Ed.) *Fourth Annual JPL Airborne Earth Science Workshop* Pasadena, CA,, JPL Publ. 93-26 Jet Propulsion Laboratory.

CLARK, R. N., SWAYZE, G.A., HEIDEBRECHT, K.B., GREEN, R.O., & GOETZ, A.F.H. (1995) Calibration to surface reflectance of terrestrial imaging spectrometry data: Comparison of methods. IN R.O.GREEN (Ed.) *Fifth Annual JPL Airborne Earth Science Workshop* Pasadena, CA,, JPL Publ. 95-1 Jet Propulsion Laboratory.

CLARK, R. N., SWAYZE, G.A., LIVO, K.E., KOKALY, R.F., KING, T.V.V., DALTON, J.B., VANCEJ.S., ROCKWELL, B.W., HOEFEN, T. & MCDOUGAL, R.R. (2002) Surface Reflectance Calibration of Terrestrial Imaging Spectroscopy Data: a Tutorial Using AVIRIS. *10th AVIRIS Airborne Geoscience Workshop Proceedings.* JPL Publication 02-1.

CLARK, R. N. & KING, T.V.V (1987) Causes of spurious features in spectral reflectance data. IN VANE, G. (Ed.) *In Proceedings of the third Airborne Imaging Spectrometer Data Analysis Workshop.* Pasadena, CA,, JPL Publ. 87-30 Jet

Propulsion Laboratory.

CONEL, J. E., & ALLEY, R.E. (1985) Lisbon Valley, Utah, Uranium Test Site Report. IN PALEY, H. N. (Ed.). Joint NASA / Geosat Test Case Project.

CONEL, J. E., GREEN, R.O., VANE, G., BRUEGGE, C.J. & ALLEY, R.E. (1987) AIS-2 radiometry and a comparison of methods for the recovery of ground reflectance. IN VANE, G. (Ed.) *In Proceedings of the third Airborne Imaging Spectrometer Data Analysis Workshop*. Pasadena, CA,, JPL Publ. 87-30 Jet Propulsion Laboratory.

DINGUIRARD, M. & SLATER, P. N. (1999) Calibration of Space-Multispectral Imaging Sensors: A Review. *Remote Sensing of Environment,* 68**,** 194-205.

DWYER, J. L., KRUSE, F.A. & LEFKOFF, A.B. (1995) Effects of empirical versus model based reflectance calibration on automated analysis of imaging spectrometer data: a case study from the Drum mountains, Utah. *Photogrammetric Engineering and Remote Sensing,* 61**,** 1247-1254.

ESA, (2004) SPECTRA. In BATTRICK, B. (Ed.). ESA Publication Division, The Netherlands, ESA. SP-1297(2).

FARRAND, W. H., SINGER, R. B. & MERÉNYI, E. (1994) Retrieval of apparent surface reflectance from AVIRIS data: A comparison of empirical line, radiative transfer, and spectral mixture methods. *Remote Sensing of Environment,* 47**,** 311-321.

FERRIER, G. & WADGE, G. (1996) The application of imaging spectrometry data to mapping alteration zones associated with gold mineralization in southern Spain. *International Journal of Remote Sensing,* 17**,** 331 - 350.

FREEANTLE, J. R., PU, R., & MILLER, J.R. (1992) Calibration of imaging spectrometer data to reflectance using pseudo-invariant features. *Proceedings of the 15th Canadian Symposium on Remote Sensing.* Toronto, Canada.

GAO, B-C., HEIDEBRECHT, K. B. & GOETZ, A. F. H. (1993) Derivation of scaled surface reflectance from AVIRIS data. *Remote Sensing of Environment,* 44**,** 165-178.

GAO, B-C., DAVIS, C., & GOETZ, A. (2006) A Review of Atmospheric Correction Techniques for Hyperspectral Remote Sensing of Land Surfaces and Ocean Color. *Geoscience and Remote Sensing Symposium, IGRASS 2006***,** 1979-1981.

GOETZ, A. F. H. KINDEL, B.C. FERRI, M. & QU, Z. (2003) HATCH: results from simulated radiances, AVIRIS and Hyperion. *Geoscience and Remote Sensing, IEEE Transactions on,* 41**,** 1215-1222.

GREEN, R. O., EASTWOOD, M. L., SARTURE, C. M., CHRIEN, T. G., ARONSSON, M., CHIPPENDALE, B. J., FAUST, J. A., PAVRI, B. E., CHOVIT, C. J., SOLIS, M. S., OLAH, M. R. & WILLIAMS, O. (1998) Imaging spectroscopy and the Airborne Visible Infrared Imaging Spectrometer (AVIRIS). *Remote Sensing of Environment,* 65**,** 227-248.

GUANTER, L., ESTELLÉS, V. & MORENO, J. (2007) Spectral calibration and atmospheric correction of ultra-fine spectral and spatial resolution remote sensing data. Application to CASI-1500 data. *Remote Sensing of Environment,* 109**,** 54-65.

HADLEY, B. C., GARCIA-QUIJANO, M., JENSEN, J. R. & TULLIS, J. A. (2005) Empirical versus Model-based Atmospheric Correction of Digital Airborne Imaging Spectrometer Hyperspectral Data. *Geocarto International,* 20**,** 21 - 28.

JENSEN, J. R. (2005) *Introductory digital image processing: a remote sensing perspective.* 3rd ed. Upper Saddle River, Prentice-Hall.

KARPOUZLI, E. & MALTHUS, T. (2003) The empirical line method for the atmospheric correction of IKONOS imagery. *International Journal of Remote Sensing,* 24**,** 1143 - 1150.

KAUFMAN, Y. J. (1989) *The atmospheric effect on remote sensing and its correction. In*: ASRAR, G., ed. *Theory and applications of optical remote sensing.* New York, Wiley. p 336-428

KAUFMAN, Y. J. & SENDRA, C. (1988) Algorithm for automatic atmospheric corrections to visible and near-IR satellite imagery. *International Journal of Remote Sensing,* 9**,** 1357 - 1381.

KRUSE, F.A. (1987) Mapping hydrothermally altered rocks in the northern grapevine mountains, Nevada and California with the Airborne Imaging Spectrometer. IN VANE, G. (Ed.) *In Proceedings of the third Airborne Imaging Spectrometer Data Analysis Workshop*. Pasadena, CA,, JPL Publ. 87-30 Jet Propulsion Laboratory.

KRUSE, F.A., KIEREIN-YOUNG, K.S., & BOARDMAN, J.W. (1990) Mineral mapping at Cuprite, Nevada with a 63-channel imaging spectrometer. *Photogrammetric Engineering and Remote Sensing,* 56**,** 83-92.

LEPRIEUR, C., CARRERE, V. AND GU, X. F. (1995) Atmospheric corrections and ground reflectance recovery for Airborne Visible/Infrared Imaging Spectrometer (AVIRIS) data: MAC Europe '91. *Photogrammetric Engineering and Remote Sensing,* 61**,** 1233-1238.

LIANG, S. (2004) *Quantitative Remote Sensing of Land Surfaces*, Hoboken, Wiley & Sons.

LIANG, S. & FANG, H. (2004) An improved atmospheric correction algorithm for hyperspectral remotely sensed imagery. *IEEE Geoscience and Remote Sensing Letters,* 1**,** 112-117.

MIESCH, C. P., L. ACHARD, V. BRIOTTET, X. LENOT, X. & BOUCHER, Y. (2005) Direct and inverse radiative transfer solutions for visible and near-infrared hyperspectral imagery. *Geoscience and Remote Sensing, IEEE Transactions on,* 43**,** 1552-1562.

MILLER, C. J. (2002) Performance assessment of ACORN atmospheric correction algorithm. *Proceedings of SPIE Conference on Algorithms and Technologies for Multispectral, Hyperspectral and Ultraspectral Imagery* VIII, Aerosense, Orlando, FL.

MILTON, E. J., FOX, N., & MACKIN, S. (2004) Calibration, Validation and the NERC Airborne Remote Sensing Facility. *Annual Conference of the Remote Sensing and Photogrammetry Society.* Nottingham, UK, Remote Sensing and Photogrammetry Society.

MILTON, E. J., SCHAEPMAN, M.E., ANDERSON, K., KNEUBUHLER, M., & FOX, N. (2007) Progress in field spectroscopy. *Remote Sensing of Environment (doi:10.1016/j.rse.2007.08.001 (http://dx.doi.org/doi:10.1016/j.rse.2007.08.001) (In Press)* 1-18.

MILTON, E. J. & NCAVEO PARTNERSHIP. (2008) The Network for Calibration and

Validation in Earth Observation (NCAVEO) 2006 Field Campaign. *Proceedings of the Remote Sensing and Photogrammetry Society Conference 2008.* Exeter, UK, Remote Sensing and Photogrammetry Society.

MORAN, M. S., BRYANT, R., THOME, K., NI, W., NOUVELLON, Y., GONZALEZ-DUGO, M. P., QI, J. & CLARKE, T. R. (2001) A refined empirical line approach for reflectance factor retrieval from Landsat-5 TM and Landsat-7 ETM+. *Remote Sensing of Environment,* 78**,** 71-82.

MORAN, M. S., JACKSON, R. D., SLATER, P. N. & TEILLET, P. M. (1992) Evaluation of simplified procedures for retrieval of land surface reflectance factors from satellite sensor output. *Remote Sensing of Environment,* 41**,** 169-184.

MORISETTE, J. T., PRIVETTE, J. L. & JUSTICE, C. O. (2002) A framework for the validation of MODIS Land products. *Remote Sensing of Environment,* 83**,** 77-96.

MORISETTE, J. T., BARET, F., PRIVETTE, J. L., MYNENI, R. B., NICKESON, J. E., GARRIGUES, S., SHABANOV, N. V., WEISS, M., FERNANDES, R. A., LEBLANC, S. G., KALACSKA, M., SANCHEZ-AZOFEIFA, G. A., CHUBEY, M., RIVARD, B., STENBERG, P., RAUTIAINEN, M., VOIPIO, P., MANNINEN, T., PILANT, A. N., LEWIS, T. E., IIAMES, J. S., COLOMBO, R., MERONI, M., BUSETTO, L., COHEN, W. B., TURNER, D. P., WARNER, E. D., PETERSEN, G. W., SEUFERT, G., COOK, R. (2006) Validation of global moderate-resolution LAI products: a framework proposed within the CEOS land product validation subgroup. *Geoscience and Remote Sensing, IEEE Transactions on,* 44**,** 1804-1817.

OUAIDRARI, H. & VERMOTE, E. F. (1999) Operational Atmospheric Correction of Landsat TM Data. *Remote Sensing of Environment,* 70**,** 4-15.

POTTER, C., KLOOSTER, S., MYNENI, R., GENOVESE, V., TAN, P.-N. & KUMAR, V. (2003) Continental-scale comparisons of terrestrial carbon sinks estimated from satellite data and ecosystem modeling 1982-1998. *Global and Planetary Change,* 39**,** 201-213.

PRICE, R., ANGER,C. D., AND MAH, S. (1995) Preliminary evaluation of CASI preprocessing techniques. *Proceedings of the 17th Canadian Symposium on Remote Sensing.* Saskatoon, Canada.

QU, Z., GOETZ, A.F.H. AND HEIDEBRECHT,K.B. (2000) High-accuracy atmosphere correction for hyperspectral data (HATCH). IN GREEN, R. O. (Ed.) *In Sumeries of the Ninth Annual JPL Airborne Earth Science Workshop.* Pasadena, CA,, JPL Publ. 00-18. Jet Propulsion Laboratory.

RAYLEIGH, LORD. (STRUTT. J. W.) (1871) *Philosophical Magazine,* 41**,** 107-274.

RICHTER, R. (2008) Atmospheric /Topographic correction for airborne imgery: ATCOR 4 User Guide. *DLR IB 565-02/08.* Wessling, Germany.

RICHTER, R. & SCHLAPFER, D. (2002) Geo-atmospheric processing of airborne imaging spectrometry data. Part 2: atmospheric/topographic correction. *International Journal of Remote Sensing,* 23**,** 2631 - 2649.

RIEDMANN, M. (2003) *Band selection using hyperspectral data from airborne and satellite sensors*. (PhD).School of Geography, University of Southampton.

ROBERTS, D. A., YAMAGUCHI, Y AND LYON, R. J. P. (1986) Comparison of various techniques for calibration of AIS data. In VANE, G. & GOETZ, A.F.H (Ed.) *In Proceedings of the second Airborne Imaging Spectrometer Data Analysis Workshop*. Pasadena, CA,, JPL Publ. 00-18 Jet Propulsion Laboratory.

ROLLIN, E. M., MILTON, E. J. & ANDERSON, K. (2002) The role of field spectroscopy in airborne sensor calibration: the example of the NERC CASI. *Proceedings of a conference on Field Spectral Measurements in Remote Sensing*. Southampton, UK, University of Southampton, School of Geography.

SCHLAPFER, D., BOJINSKI, S., SCHAEPMAN, M. & RICHTER, R (2000) Combination of geometric and atmospheric correction for AVIRIS data in rugged terrain. In GREEN, R. O. (Ed.) *In Summaries of the Ninth Annual JPL Airborne Earth Science Workshop*. Pasadena, CA,, JPL Publ. 00-18. Jet Propulsion Laboratory.

SHARMA, A. R., BADARINATH, K. V. S. & ROY, P. S. (2009) Comparison of ground reflectance measurement with satellite derived atmospherically corrected reflectance: A case study over semi-arid landscape. *Advances in Space Research,* 43**,** 56-64.

SMITH, G. M. & MILTON, E. J. (1999) The use of the empirical line method to calibrate remotely sensed data to reflectance. *International Journal of Remote Sensing,* 20**,** 2653-2662.

STAENZ, K., SECKER, J., GAO, B. C., DAVIS, C. & NADEAU, C. (2002) Radiative transfer codes applied to hyperspectral data for the retrieval of surface reflectance. *ISPRS Journal of Photogrammetry and Remote Sensing,* 57**,** 194-203.

STRAHLER, A., BOSCHETTI, L., FOODY, G. M., FRIEDL, M. A., HANSEN, M. C., HEROLD, M., MAYAUX, P., MORISETTE, J. T., STEHMAN, V., & WOODCOCK, C. E. (2006) Global Land Cover Validation: Recommendations for Evaluation and Accuracy Assessment of Global Land Cover Maps. Luxemburg, Publication of the European Communities, European Commission.

TEILLET, P. M., FEDOSEJEVS, G., HAWKINS, R. K., LUKOWSKI, T. I., NEVILLE, R. A., STAENZ, K., TOUZI, R., SANDEN, J., VAN DER. & WOLFE,J. (2004) Importance of Data Standardization for Generating High Quality Earth Observation Products for Natural Resource Management. Canada Centre for Remote Sensing

TEILLET, P. M., FEDOSEJEVS, G., GAUTHIER, R. P., O'NEILL, N. T., THOME, K. J., BIGGAR, S. F., RIPLEY, H. & MEYGRET, A. (2001) A generalized approach to the vicarious calibration of multiple Earth observation sensors using hyperspectral data. *Remote Sensing of Environment,* 77**,** 304-327.

TEILLET, P. M., FEDOSEJEVS, G., GAUTHIER, R. P., SHIN, R. T., O'NEILL, N. T., THOME, K. J., BIGGAR, S. F., RIPLEY, H. & MEYGRET, A. (1999) Radiometric calibration of multiple Earth observation sensors using airborne hyperspectral data at the Newell County rangeland test site. IN BARNES, W. L. (Ed.) *Earth Observing Systems Iv.* Bellingham, Spie - Int Soc Optical Engineering.

TEILLET, P. M., SLATER, P. N., DING, Y., SANTER, R. P., JACKSON, R. D. & MORAN, M. S. (1990) Three methods for the absolute calibration of the NOAA AVHRR sensors in-flight. *Remote Sensing of Environment,* 31**,** 105-120.

VAN DER MEER, F. (1994) Extraction of mineral absorption features from high-spectral resolution data using non-parametric geostatistical techniques. *International Journal of Remote Sensing,* 15**,** 2193 - 2214.

ZAGOLSKI, F. & GASTELLU-ETCHEGORRY, J. P. (1995) Atmospheric corrections of AVIRIS images with a procedure based on the inversion of the 58 model. *International Journal of Remote Sensing,* 16**,** 3115 - 3146.

Online Resources:

NCAVEO, *Online.* Available: http://www.ncaveo.ac.uk/overview/. [accessed 2009, January17*]*.

MODIS LAND VALIDATION STRATEGY, *Online.* Available: http://landval.gsfc.nasa.gov/index.html. [Accessed 2009, January18].

LAND PRODUCT VALIDATION, *Online.* Available: http://lpvs.gsfc.nasa.gov/. [Accessed 2009, January18].

Unpublished Resource:

ANANDAKUMAR, R. M. (2008) *Effect of the atmosphere on object-oriented segmentation for land cover classification.* (MSc). School of Geography, University of Southampton.

APPENDICES

Appendix-A. SPOT-5 HRG camera specification.

(Source: http://spot5.cnes.fr/gb/satellite/camerasHRG.htm accessed on 2009, Jan 25)

HRG technical data			
Mass	356 Kg		
Maximum power (depending on mode)	344 w		
Dimensions	2.65 x 1.42 x 0.96 m		
Oblique viewing angle	+/- 27 degrees		
Focal length	1.082 m		
Field of view	+/- 2 degrees		
Performance	P	B1 B2 B3	SWIR
Spectral range (panchromatic band)	0,49-0,69 microns	B1 0.50-0.59 B2 0.61-0.68 B3 0.78-0.89	1.58-1.75 microns
Detectors per line	12000	6000	3000
Number of lines	2 offset	3 registered	1
Detector pitch	6.5 microns	13 microns	26 microns
Integration time per line	0.752 ms	1.504 ms	3.008 ms
Ground sample distance	5 x 5 m single image 3,5 x 3,5 dual image	10 x 10 m	20 x 20 m
Signal-to-noise ratio	170	240	230
Modulation transfer function	> 0.2	> 0.3	> 0.2

Appendix-B. CASI-2 Specification.

(Source : NERC-ARSF)

Parameter	Description
IFOV (Instantaneous Field Of View)	
Across Tack	54.4 ° (custom lens)
Along track	0.1151 °
Aperture	f/2.8 - f/11 (Automated iris control)
Spectral range	405 - 950 nm
Spatial samples	512 spatial pixels
Spectral samples	288 at 1.8nm intervals (2.2nm FWHM @ 650nm)
Dynamic range	12-bits (4096 levels)
Recording	1 removable 9 GByte Hard Disk
Operating Modes	
• Spatial Mode	512 pixels across swath, up to 18 spectral bands (fully programmable).
• Spectral Mode	full spectrum (288 channels) for up to 39 look directions spread across swath (4, 8, 12, or 16 pixel spacing between look directions). Includes a monochromatic image at full spatial resolution (Scene Recovery Channel).
• Enhanced Spectral Mode	full spectrum (288 channels) in a block of 101 adjacent spatial pixels.
• Full Frame	512 pixels across swath x 288 spectral pixels (~1-2 sec. Integration time limits use to laboratory calibration or ground-based field use).
Downwelling Incident Light Sensor (ILS)	
Lumogen coating for enhancement of blue response below 450nm	

Appendix-C. SPECIM AISA-Eagle Specification.

(Source : OEM technical data sheet)

OPTICAL CHARACTERISTICS	TYPICAL SPECIFICATIONS
Spectrograph	High efficiency transmissive imaging spectrograph. Throughput practically independent of polarization. Smile and keystone < 2 microns.
F/#	F/2.4
Spectral range	400-970 nm
Spectral resolution	2.9 nm
Slit width	30 microns
FODIS (optional)	Diffuse down welling irradiance collector and fiber optic cable (5 m standard) with SMA connector
Calibration	Sensor provided with wavelength and radiometric calibration file.

FORE OPTICS			
Fore optics options	OLE23	OLE18.5	OLE9
Focal length	23 mm	18.5 mm	Wide FOV lens More specifications upon request
FOV	29.9 degrees	37.7 degrees	
IFOV	0.029 degrees	0.037 degrees	
Swath width	0.53 x altitude	0.68 x altitude	
Ground resolution @ 1000 m altitude	0.52 m	0.68 m	

ELECTRICAL CHARACTERISTICS				
Camera	Progressive scan CCD camera			
Spectral binning options	1x	2x	4x	8x
# of spectral bands	488	244	122	60
Spectral sampling/band	1.25 nm	2.3nm	4.6nm	9.2nm
Image rate, up to (images/s)	30	50	100	160
Spatial pixels, up to	1024, of which 70 - 80 FODIS pixels (optional)			
Output	12 bits digital			
SNR	350:1 - 1400:1 (depending on the band configuration) More detailed SNR data in various conditions available from SPECIM.			
Integration time	Adjustable, independent of image rate			
Shutter	Electromechanical shutter for dark background registration, user-controllable by software.			
Operating modes	Hyperspectral and multispectral The operator can create application specific band configurations, and quickly change from one mode or configuration to others in flight operation.			
Power consumption				
Complete system with rack PC	435 W			
Complete system with lightweight PC	315 W			

Swath width vs altitude

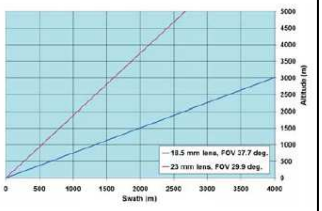

Ground pixel size vs. altitude

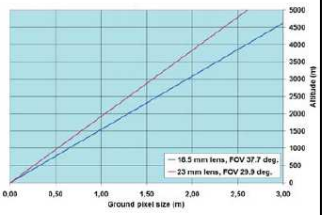

Image rate at aircraft velocity of 60 m/s (120 knots)

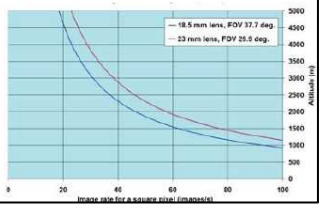

Appendix-D. Summery of flight mission and time line

. (source: NEODC and office of NCAVEO)

Proj No.	GB06-10	Proj Name	NCAVEO	PI	A.K. Wilson	Do-228	D-CALM	Date	17.06.2006	Day	168	Land	12:30
Pilot	Carl Joseph	Co Pilot	David Davies	Op	Simon Roberts	Base	Kidlington	Sortie		Log		Take off	09:50
Observer		Weather	Cloudy and hazy					QNH	1020 Mb	OAT	23ºC	Total	2:40

Site parameters required		*casi* 2 RHD = C	ATM RHD = 4		WILD RC-10	Nav card = B	LiDAR Settings	Eagle RHD	Chock Time	
Gnd speed kts	135	Config Veg	Ref Temps		Filter = y	F. stop 5.6	LiDAR RHD = 1	Scan Angle 20	Hawk RHD	Engine's
Alt ft angl	6250		BB1	15	Film AGFA colour		Film #	Scan Freq 20	E fps 30 IT 12	On 09:40
Pixel size m	2.5m	Mode Spatial	BB2	35	Shutter speed 320		Cassette #	Resolution 1.4	H fps 30 IT 15	Off 12:37

General nav. information				*casi* 2			ATM			IDS	RC – 10		Time (GMT)		GPS Quality		Drop Outs (%)	Eagle	Hawk	Notes
Line No.	Dir	GPS Alt ft	Spd kts	File No	F	IT ms	Scan x 100 Start	Stop	Scn Spd	File No	Frame No's	Tot.	Start	Stop	PDOP	SVs		File No	File No	
Test				001	3	50			25	001	-		:	:				1-1	1-1	Dark
7	148	5470	136	002	3	42			25		-		10:40	10:45	2.25	7	0	1-2	1-2	
6	328	5290	134	003	3	42					-		10:50	10:55	2.40	7	0	1-3	1-3	E = 31 H = 13
5	148	5320	137	004	3	42					-		10:58	11:03	2.58	7	0	1-4	1-4	
4	328	5290	136	005	3	42					-		11:06	11:12	1.71	8	0	1-5	1-5	
3	148	5320	134	006	3	42					-		11:15	11:19	1.74	8	0	1-6	1-6	
2	328	5220	135	007	3	42					-		11:22	11:27	1.43	10	0	1-7	1-7	
1	148	5240	132	008	3	42					-		11:30	11:35	1.61	9	0	1-8	1-8	
X	061	5230	130	009	3	42					-		11:41	11:43	1.76	9	0	1-9	1-9	
											-									
8	148	5250	133	010	3	42					-		11:49	11:54	1.84	9	0	1-10	1-10	
9	328	5330	137	011	3	42					-		11:57	12:01	1.89	9	0	1-11	1-11	
											-		:	:						
Test				012							-		:	:				1-12	1-12	Dark
											-		:	:						
											-		:	:						
											-		:	:						
											-		:	:						
											-		:	:						
											-		:	:						

	Cloud cover	Shadow effects	Illumination	Turbulence/ Speed issues	Other
1	0-10% ☐	0-10% ☐	>90% ☐	None ☐	
2	10-20% ☐	10-20% ☐	90-80% X	Slight X	Spacing 556 Swath 744
3	20-30% X	20-30% X	80-70% ☐	Variable ☐	480 642
4	30-40% ☐	30-40% ☐	70-60% ☐	High ☐	
5	40-50% ☐	40-50% ☐	60-50% ☐	Excessive ☐	
6	50-60% ☐	50-60% ☐	50-40% ☐		
7	60-70% ☐	60-70% ☐	40-30% ☐		
8	70-80% ☐	70-80% ☐	30-20% ☐		
9	80-90% ☐	80-90% ☐	20-10% ☐		
10	>90% ☐	>90% ☐	10-0% ☐		

Overall data quality this sortie: 4

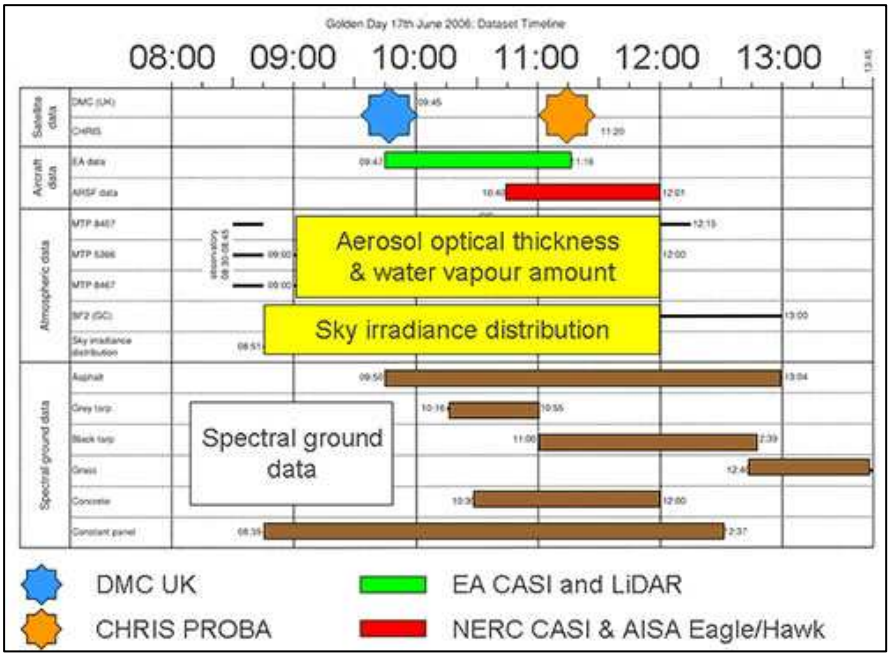

Appendix-E. Data level supplied by NERC-ARSF.

(source: NERC-ARSF, http://arsf.nerc.ac.uk/data/)

Product	Definition
Level 0	Raw "sensor format" data at original resolution
Level 1a	Level 0 data reformatted to image files with ancillary files appended
Level 1b	Level 1a data to which radiometric calibration algorithms have been applied, to produce radiance or irradiance, and to which location and navigational information has been appended.
Level 2	Geophysical or environmental parameters derived from Level 1a or 1b data, may include atmospheric correction.
Level 3a	Level 1b or 2 data mapped to a geographic co-ordinate system using on-board attitude and positional information only.
Level 3b	Level 1b or 2 data mapped to a geographic co-ordinate system using on-board attitude and positional information with additional ground control points.
Level 4	Multi-temporal/multi-sensor gridded data products.

Appendix-F. AZGCORR and AZEXHDF commands

AZGCORR and AZEXHDF commands used and their explanations

Commands used to correct Eagle data:

- `azgcorr -v -in -l 5513 6277 -cspacM -mUK99 osgb02.txt -be -p 1.0 1.0 -1 e168051b.hdf -3 e16805sub3a.hdf -eh chilbolton_5m.dem`
- `azexhdf –h e16805sset3a.hdf –G e16805sset3a.tif`

Commands used to correct CASI:

- `azgcorr -v -be -l 4202 4729 -p 2.0 2.0 -1 c168051b.hdf -3a c16805sset3a.hdf -mUK99 osgb02.txt -eh chilbolton_5m.dem`
- `azexhdf –h e16805sset3a.hdf –G e16805sset3a.tif`

The parameters are explained below; however the variable such as line number and file name will change for Eagle and CASI

Commands	Azgcorr Function
Azgcorr	Basic parameter which launches the programme
-v	Runs in verbose mode
-in	Nearest Neighborhood interpolation
-l (small L)	Line start and end option to work on a subset defined by 5513 to 6277
-cspacM	A new projection correction algorithm which has been incorporated in the new version. Not necessary while working with the latest version (pers. Comm., 2008)
-mUK99	Changes map projection to UK National grid 1999 method
Osgb02	It's the Ordnance Survey projection correction file, which needs to be included
-be	A new band editing function if any bad lines in some bands appeared which has been incorporated in the new version. Not necessary while working with the latest version (pers. Comm., 2008)

Commands	Azgcorr Function
-p	Pixel dimension in metre
-1 (number)	Calls the input image (Level-1)
-3	The output image (Level-3)
-eh	Calls the DEM flat file with header information
chilbolton_5m.dem	5 metre Digital Surface Model file which needs to be included for z correction.
Commands	**Azexhdf Function**
Azexhdf	Basic parameter which launches the programme
-h	Input HDF file
-G	Convert Level-3 image data to Geotiff file (.tif)

Appendix-G. Four Homogenous ROIs

The four ROIs from where 995 random pixels from both the CASI-2 and Eagle were collected

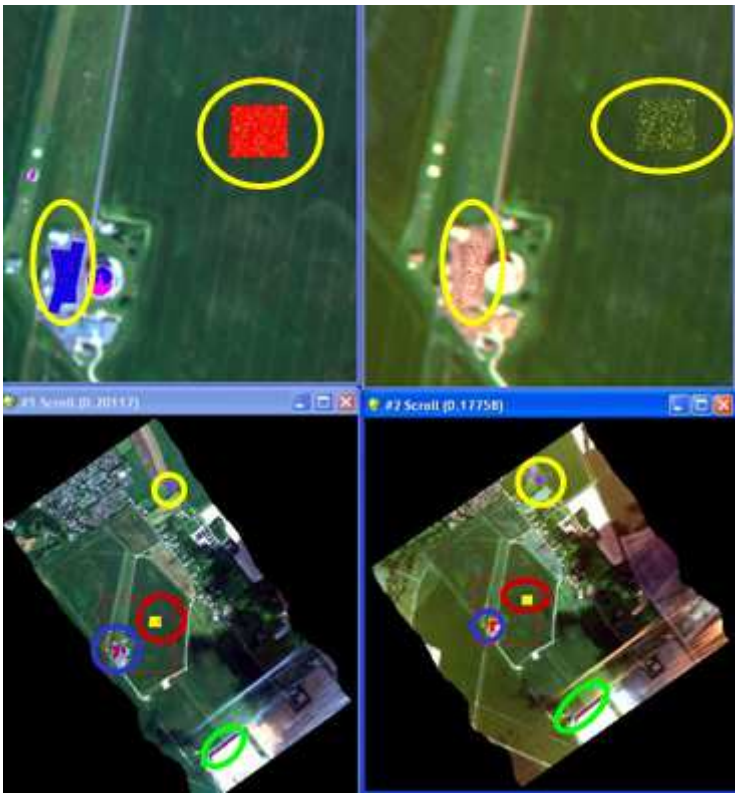

Left part is the Eagle subset and the right side CASI-2 subset. The four coloured rings below shows the four ROIs. Green is fallow land, blue is asphalt, red is grass-1 and yellow is grass-2. The top part of the image shows a magnified view of random samples from the asphalt and grass ROI.

Appendix-H. Tips and Tricks with ATCOR-4

Tips and Tricks with ATCOR 4.

The following are from my experience encountered while working with ATCOR 4 in an x7 Linux server multiple user network system and also with a desktop running on Windows XP operating system. The way around devised are not necessarily the most efficient or logical and do not guarantee working on other systems. The novice but interested users of ATCOR 4 might find these tips and tricks useful.

1. It is felt ATCOR 4 is uniquely suited for scientific R&D but not de-facto choice for production environment.

2. Multiuser Linux based network system proved to be instable with many glitches with setting up permission and occasional bailing out from the programme. It is recommended to use single user with all permission desktop version (Linux, Unix or Windows)

3. It is felt there lies enough scope for improvement in manual and on-line help.

4. RESLUT operation resamples the required monochromatic 'atm_database' and allows selection of flight altitude region but not at the required flight altitude. To interpolate at that required height the way around found was firstly select the "Atmospheric file" with required aerosol type and a flying height close to the required one, secondly click on "Aerosol Type" then "Visib Estimate" and thirdly return back to "Atmospheric file" and select the interpolated file from the drop down list.

5. After entering "Spectra" Module, it is worthwhile to check whether the required "atmospheric file" is selected, if not return and repeat.

6. If spectral calibration has to be performed, it is advisable to bail out completely from the programme after it. I also used to delete the previous process initialisation file (*.ini) and re-write the specification of all processing parameters.

….. cont

7. Without entering the main panel all previous response file, (.cal), (.wvl) and LUT file from the respective folder (‘sensor’ and ‘atm_lib’) in ATCOR4 directory needs to be deleted and be replaced with the new (.cal) and (.wvl) file. Again new response file and new RESLUT has to be created. Upon entering main panel make sure to select the right updated “Calibration file” and the wavelength file.

8. After all processing parameter is set up clicking the “In-flight Calibration” might give error, check whether the new cal file is selected, click on “Aerosol Type” then “Visib Estimate” and return back to “Atmospheric file” to check the right interpolated file from the drop down list is selected. Sometimes an option of requisite water vapour might appear which could be because of wrong selection of atmosphere file or could also get changed even if rightly selected. Check again and select the right water vapour used during spectral calibration. Make sure to bail out of programme, replace the previous with the new (.cal) file delete the previous (.ini) file repeat step 7 and run the final image processing.

Appendix-I. Spectral and Radiometric Calibration

Results from spectral and radiometric calibration during RTGC USGS correction:

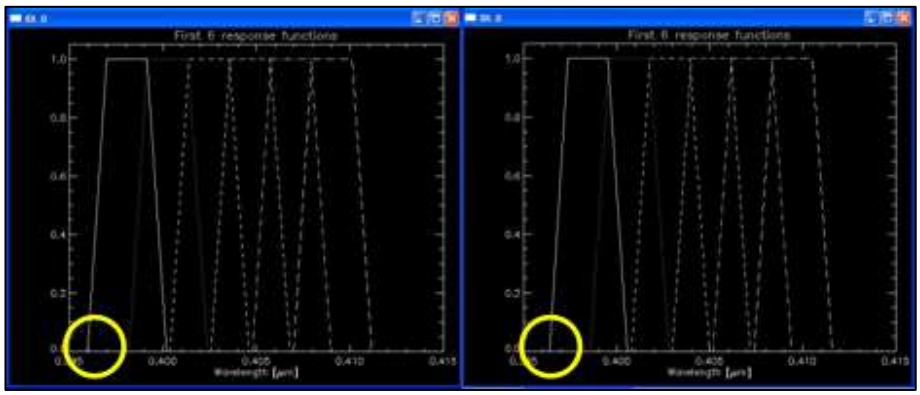

Shift in spectral calibration in the first six response function after spectral calibration

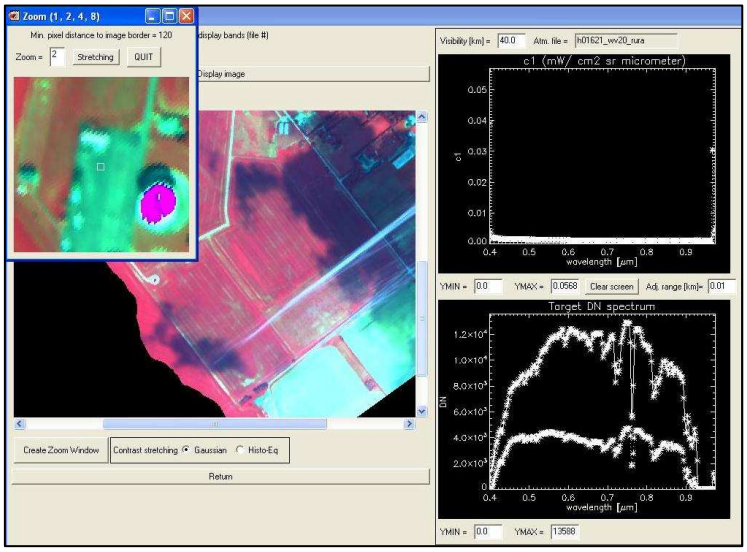

Radiometric calibration of the Eagle generated

Appendix-J. Atmospheric correction of Eagle data

Result from atmospheric correction using RTGC method

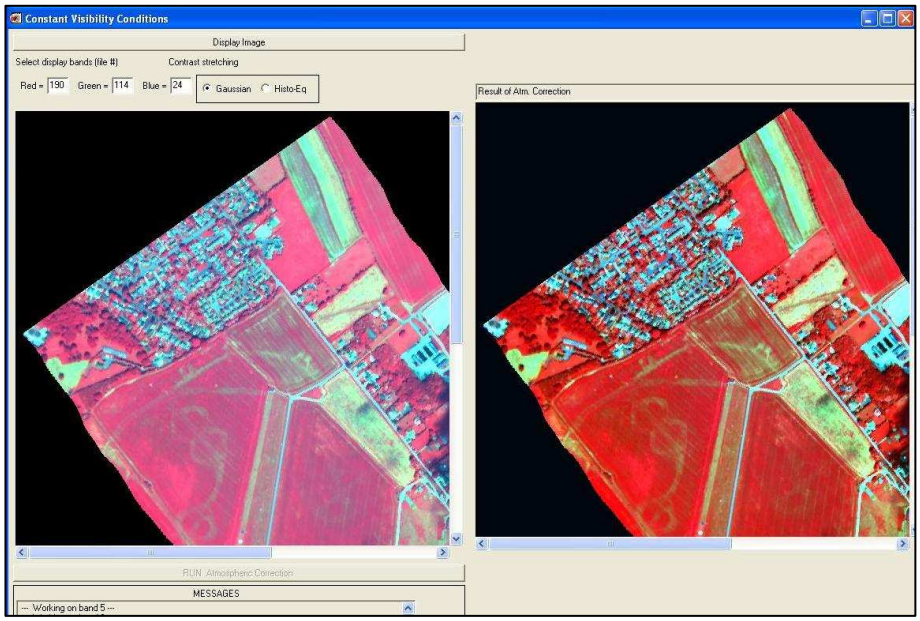

The display on the right side window shows the result of atmospheric correction on Eagle data for the study area.

Appendix-K. t-test in evaluation of Eagle calibration

```
GET
  FILE='D:\GEM_studymat\5.MSc Thesis\Analysis
Output\SPSS\NL_output\Masterc'+
 'opy_independent.sav'.
DATASET NAME DataSet1 WINDOW=FRONT.
T-TEST
  GROUPS = ROI_code(1 2)
  /MISSING = ANALYSIS
  /VARIABLES = CASI_0.4512 CASI_0.4914 CASI_0.5535 CASI_0.6095
CASI_0.6524
  CASI_0.6724 CASI_0.7031 CASI_0.7126 CASI_0.7433 CASI_0.752
CASI_0.7645
  CASI_0.7828 CASI_0.8221 CASI_0.8664 CASI_0.9413
  /CRITERIA = CI(.95) .
T-Test
```

Output Created		17-JAN-2009 19:19:40
Comments		
Input	Data	D:\GEM_studymat\5.MSc Thesis\Analysis Output\SPSS\NL_output\Mastercopy_independent.sav
	Active Dataset	DataSet1
	Filter	<none>
	Weight	<none>
	Split File	<none>
	N of Rows in Working Data File	1990
Missing Value Handling	Definition of Missing	User defined missing values are treated as missing.
	Cases Used	Statistics for each analysis are based on the cases with no missing or out-of-range data for any variable in the analysis.
Syntax		T-TEST GROUPS = ROI_code(1 2) /MISSING = ANALYSIS /VARIABLES = CASI_0.4512 CASI_0.4914 CASI_0.5535 CASI_0.6095 CASI_0.6524 CASI_0.6724 CASI_0.7031 CASI_0.7126 CASI_0.7433 CASI_0.752 CASI_0.7645 CASI_0.7828 CASI_0.8221 CASI_0.8664 CASI_0.9413 /CRITERIA = CI(.95) .

Resources	Processor Time	0:00:00.16
	Elapsed Time	0:00:00.09

Notes

```
[DataSet1] D:\GEM_studymat\5.MSc Thesis\Analysis
Output\SPSS\NL_output\Mastercopy_independent.sav
```

Group Statistics

	ROI_code	N	Mean	Std. Deviation	Std. Error Mean
CASI_0.4512	1	995	3840.9276	844.09630	26.75965
	2	995	2943.9896	893.51696	28.32639
CASI_0.4914	1	995	3863.3156	1097.78509	34.80213
	2	995	3238.1738	1095.72190	34.73672
CASI_0.5535	1	995	4930.6412	1114.68430	35.33787
	2	995	4660.1490	1109.55822	35.17536
CASI_0.6095	1	995	4385.8392	1685.53715	53.43512
	2	995	4086.6579	1666.71921	52.83855
CASI_0.6524	1	995	3893.8844	1932.72244	61.27142
	2	995	3428.2800	1848.36578	58.59713
CASI_0.6724	1	995	3957.8492	2195.88863	69.61435
	2	995	3478.3260	2088.18575	66.19994
CASI_0.7031	1	995	4829.9367	1690.80202	53.60203
	2	995	4462.3345	1589.28681	50.38378
CASI_0.7126	1	995	6092.4482	1623.70328	51.47485
	2	995	5559.6796	1539.92944	48.81905
CASI_0.7433	1	995	9990.6814	2838.59810	89.98961
	2	995	9474.0495	2842.83369	90.12389
CASI_0.752	1	995	10944.9709	3210.60885	101.78314
	2	995	10080.5509	3106.95731	98.49717
CASI_0.7645	1	995	5368.2271	1510.15256	47.87505
	2	995	6228.2555	1956.73969	62.03282
CASI_0.7828	1	995	11319.3628	3336.32021	105.76846
	2	995	10100.1170	3147.04032	99.76789
CASI_0.8221	1	995	7938.2000	2218.77930	70.34003
	2	995	6702.8052	2203.54834	69.85718
CASI_0.8664	1	995	10498.3508	2792.73987	88.53581
	2	995	8149.8702	2588.81780	82.07104
CASI_0.9413	1	995	2639.8884	460.28845	14.59212
	2	995	.0001	.00016	.00001

Independent Samples Test

		Levene's Test for Equality of Variances		t-test for Equality of Means						
		F	Sig.	t	df	Sig. (2-tailed)	Mean Difference	Std. Error Difference	95% Confidence Interval of the Difference	
		Lower	Upper	Lower	Upper	Lower	Upper	Lower	Upper	Lower
CASI_0 .4512	Equal variances assumed	34.272	.000	23.018	1988	.000	896.93799	38.96747	820.51664	973.35935
	Equal variances not assumed			23.018	1981.598	.000	896.93799	38.96747	820.51648	973.35950
CASI_0 .4914	Equal variances assumed	1.072	.301	12.714	1988	.000	625.14174	49.17141	528.70883	721.57465
	Equal variances not assumed			12.714	1987.993	.000	625.14174	49.17141	528.70883	721.57465
CASI_0 .5535	Equal variances assumed	.103	.748	5.425	1988	.000	270.49221	49.86051	172.70787	368.27656
	Equal variances not assumed			5.425	1987.958	.000	270.49221	49.86051	172.70787	368.27656
CASI_0 .6095	Equal variances assumed	.513	.474	3.981	1988	.000	299.18130	75.14802	151.80417	446.55844
	Equal variances not assumed			3.981	1987.749	.000	299.18130	75.14802	151.80416	446.55845
CASI_0 .6524	Equal variances assumed	1.176	.278	5.492	1988	.000	465.60445	84.78096	299.33559	631.87330
	Equal variances not assumed			5.492	1984.054	.000	465.60445	84.78096	299.33539	631.87351
CASI_0 .6724	Equal variances assumed	2.251	.134	4.992	1988	.000	479.52327	96.06555	291.12356	667.92299
	Equal variances not assumed			4.992	1982.993	.000	479.52327	96.06555	291.12327	667.92328
CASI_0 .7031	Equal variances assumed	2.931	.087	4.997	1988	.000	367.60217	73.56427	223.33100	511.87333
	Equal variances not assumed			4.997	1980.427	.000	367.60217	73.56427	223.33067	511.87367
CASI_0 .7126	Equal variances assumed	13.459	.000	7.510	1988	.000	532.76863	70.94336	393.63750	671.89976
	Equal variances not assumed			7.510	1982.447	.000	532.76863	70.94336	393.63726	671.90000
CASI_0 .7433	Equal variances assumed	.000	.992	4.056	1988	.000	516.63189	127.35951	266.85977	766.40401
	Equal variances not assumed			4.056	1987.996	.000	516.63189	127.35951	266.85977	766.40401
CASI_0 .752	Equal variances	1.048	.306	6.103	1988	.000	864.41997	141.63863	586.64424	1142.19569
	Equal variances not assumed			6.103	1985.863	.000	864.41997	141.63863	586.64406	1142.19588
CASI_0 .7645	Equal variances assumed	44.687	.000	-10.976	1988	.000	-860.02841	78.35874	-1013.70227	-706.35455

…cont

		Levene's Test for Equality of Variances		t-test for Equality of Means						
		F	Sig.	t	df	Sig. (2-tailed)	Mean Difference	Std. Error Difference	95% Confidence Interval of the Difference	
		Lower	Upper	Lower	Upper	Lower	Upper	Lower	Upper	Lower
	Equal variances not assumed			-10.976	1868.028	.000	-860.02841	78.35874	-1013.70828	-706.34853
CASI_0	Equal variances assumed	4.436	.035	8.386	1988	.000	1219.24586	145.39807	934.09727	1504.39444
.7828	Equal variances not assumed			8.386	1981.257	.000	1219.24586	145.39807	934.09668	1504.39503
CASI_0	Equal variances assumed	.574	.449	12.462	1988	.000	1235.39478	99.13499	1040.97541	1429.81415
.8221	Equal variances not assumed			12.462	1987.906	.000	1235.39478	99.13499	1040.97540	1429.81416
CASI_0	Equal variances assumed	8.793	.003	19.453	1988	.000	2348.48051	120.72384	2111.72199	2585.23902
.8664	Equal variances not assumed			19.453	1976.680	.000	2348.48051	120.72384	2111.72116	2585.23985
CASI_0	Equal variances	1557.954	.000	180.912	1988	.000	2639.88831	14.59212	2611.27085	2668.50577
.9413	Equal variances not assumed			180.912	994.000	.000	2639.88831	14.59212	2611.25341	2668.52322

Appendix-L. Confidence Interval on means in Data Validation

(A) Direct Validation of Eagle with Ground (Grey and Black) Targets

GREY TARGETS

Eagle				GREY TARGETS (FIELD)			
	SPOT1	SPOT2	SPOT3		SPOT1	SPOT2	SPOT3
$\bar{x}$	27.74	27.88	29.45	$\bar{x}$	30.17	29.51	28.11
SD	0.00	0.00	0.00	SD	1.18	1.17	1.12
SE	0.00	0.00	0.00	SE	0.19	0.19	0.18
t	2.04	2.04	2.04	t	2.04	2.04	2.04
(t x SE)	0.00	0.00	0.00	(t x SE)	0.39	0.39	0.38
n-1	36.00	36.00	36.00	n-1	36.00	36.00	36.00
CI_min	**27.74**	**27.88**	**29.45**	CI_min	**29.77**	**29.12**	**27.73**
CI_max	**27.74**	**27.88**	**29.45**	CI_max	**30.56**	**29.91**	**28.48**
Abs diff	-2.42	-1.63	1.34				
Rel diff	-8.03	-5.54	4.78				

BLACK TARGETS

Eagle				BLACK TARGETS (FIELD)			
	SPOT1	SPOT2	SPOT3		SPOT1	SPOT2	SPOT3
$\bar{x}$	5.06	4.80	6.85	$\bar{x}$	3.30	3.17	2.98
SD	0.00	0.00	0.01	SD	0.39	0.38	0.36
SE	0.00	0.00	0.00	SE	0.06	0.06	0.06
t	2.02	2.02	2.02	t	2.02	2.02	2.02
(t x SE)	0.00	0.00	0.00	(t x SE)	0.12	0.12	0.12
n-1	38.00	38.00	38.00	n-1	38.00	38.00	38.00
CI_min	**5.06**	**4.80**	**6.85**	CI_min	**3.18**	**3.05**	**2.86**
CI_max	**5.06**	**4.80**	**6.85**	CI_max	**3.42**	**3.29**	**3.10**
Abs diff	1.76	1.63	3.87				
Rel diff	53.47	51.46	129.82				

(B) Indirect Validation of Eagle with EA-CASI-3 Reflectance Map

GRASS							
Eagle				CASI-3			
	SPOT1	SPOT2	SPOT3		SPOT1	SPOT2	SPOT3
$\bar{x}$	3.6655	4.00875	49.2702	$\bar{x}$	4.2109	4.984	47.7472
SD	0.14939	0.12293	0.96669	SD	0.34056	0.31699	2.68067
SE	0.0334	0.02749	0.21616	SE	0.07615	0.07088	0.59942
t	2.093	2.093	2.093	t	2.093	2.093	2.093
(t x SE)	0.06992	0.05753	0.45242	(t x SE)	0.15939	0.14836	1.25458
n-1	19	19	19	n-1	19	19	19
CI_min	3.59558	3.95122	48.8177		4.05151	4.83564	46.4926
CI_max	3.73542	4.06628	49.7226		4.37029	5.13236	49.0017
Abs diff	-0.5454	-0.9752	1.523				
Rel diff	-12.9521	-19.568	3.18972				

CONCRETE							
Eagle				CASI-3			
	SPOT1	SPOT2	SPOT3		SPOT1	SPOT2	SPOT3
$\bar{x}$	25.5549	29.2675	34.2502	$\bar{x}$	24.0876	29.558	35.5683
SD	1.87316	2.33216	3.16391	SD	2.18023	2.50712	2.74848
SE	0.40876	0.50892	0.69042	SE	0.47577	0.5471	0.59977
t	2.086	2.086	2.086	t	2.086	2.086	2.086
(t x SE)	0.85267	1.06161	1.44022	(t x SE)	0.99245	1.14125	1.25112
n-1				n-1			
CI_min	24.7022	28.2059	32.8099		23.0952	28.4167	34.3171
CI_max	26.4075	30.3291	35.6904		25.0801	30.6992	36.8194
Abs diff	1.46724	-0.2905	-1.3181				
Rel diff	6.09125	-0.9827	-3.7058				

ASPHALT							
Eagle				CASI-3			
	SPOT1	SPOT2	SPOT3		SPOT1	SPOT2	SPOT3
$\bar{x}$	7.94327	11.0325	13.8623	$\bar{x}$	8.57173	9.59295	14.3762
SD	0.60273	1.63407	0.68723	SD	0.99509	1.09506	1.52246
SE	0.1285	0.34838	0.14652	SE	0.21215	0.23347	0.32459
t	2.08	2.08	2.08	t	2.08	2.08	2.08
(t x SE)	0.26729	0.72464	0.30476	(t x SE)	0.44128	0.48561	0.67515
n-1	21	21	21	n-1	21	21	21
CI_min	7.67599	10.3079	13.5575		8.13044	9.10734	13.7011
CI_max	8.21056	11.7572	14.167		9.01301	10.0786	15.0514
Abs diff	-0.62845	1.43958	-0.5139				
Rel diff	-7.33171	15.0066	-3.5749				

(C) Validation of ELM-SPOT and ATCOR-2 corrected SPOT with Eagle Reflectance map

ASPHALT											
Eagle				SPOT - ELM				SPOT - ATCOR			
	SPOT1	SPOT2	SPOT3		SPOT1	SPOT2	SPOT3		SPOT1	SPOT2	SPOT3
$\overline{X}$	9.23	10.11	15.28	$\overline{X}$	8.17	9.36	16.79	$\overline{X}$	11.87	12.71	21.32
SD	0.90	0.99	1.57	SD	0.98	1.07	3.15	SD	0.87	1.12	3.15
SE	0.20	0.22	0.34	SE	0.21	0.23	0.69	SE	0.19	0.24	0.69
t	2.09	2.09	2.09	t	2.09	2.09	2.09	t	2.09	2.09	2.09
(t x SE)	0.41	0.45	0.72	(t x SE)	0.45	0.49	1.44	(t x SE)	0.40	0.51	1.44
n-1	20.00	20.00	20.00	n-1	20.00	20.00	20.00	n-1	20.00	20.00	20.00
CI_min	8.82	9.66	14.57		7.72	8.87	15.35		11.47	12.20	19.88
CI_max	9.64	10.56	16.00		8.61	9.84	18.22		12.27	13.22	22.75
Eagle and SPOT-ELM					Eagle and SPOT- ATCOR						
Abs diff	-1.07	-0.76	1.51		Abs diff	2.64	2.60	6.03			
Rel diff	-11.55	-7.47	9.86		Rel diff	28.60	25.71	39.48			

BARE SOIL											
Eagle				SPOT - ELM				SPOT - ATCOR			
	SPOT1	SPOT2	SPOT3		SPOT1	SPOT2	SPOT3		SPOT1	SPOT2	SPOT3
$\overline{X}$	15.801	21.541	28.684	$\overline{X}$	14.414	20.627	24.045	$\overline{X}$	16.307	22.944	31.9673
SD	0.8993	1.2023	1.2581	SD	0.9407	0.7116	0.5527	SD	0.8784	0.80722	0.73381
SE	0.2844	0.3802	0.3979	SE	0.2975	0.225	0.1748	SE	0.2778	0.25526	0.23205
t	2.262	2.262	2.262	t	2.262	2.262	2.262	t	2.262	2.262	2.262
(t x SE)	0.6433	0.86	0.9	(t x SE)	0.6729	0.509	0.3953	(t x SE)	0.6283	0.57741	0.5249
n-1	9	9	9	n-1	9	9	9	n-1	9	9	9
CI_min	15.158	20.681	27.784		13.742	20.117	23.65		15.678	22.3666	31.4424
CI_max	16.444	22.401	29.584		15.087	21.136	24.441		16.935	23.5214	32.4922
Eagle and SPOT-ELM					Eagle and SPOT- ATCOR						
Abs diff	-1.3866	-0.9145	-4.6385		Abs diff	0.5056	1.403				
Rel diff	-8.7755	-4.2454	-16.171		Rel diff	3.2001	6.513				

BRIGHT VEGETATION											
	Eagle				SPOT-ELM				SPOT-ATCOR		
	SPOT1	SPOT2	SPOT3		SPOT1	SPOT2	SPOT3		SPOT1	SPOT2	SPOT3
$\overline{x}$	3.6667	3.9589	48.527		1.4707	1.4953	42.692	$\overline{x}$	6.0777	4.47558	56.4343
SD	0.2144	0.2578	2.6291	SD	0.475	0.3978	3.6986	SD	0.4527	0.45121	4.95979
SE	0.0715	0.0859	0.8764	SE	0.1583	0.1326	1.2329	SE	0.1509	0.1504	1.65326
t	2.306	2.306	2.306	t	2.306	2.306	2.306	t	2.306	2.306	2.306
(t x SE)	0.1648	0.1982	2.0209	(t x SE)	0.3651	0.3058	2.843	(t x SE)	0.348	0.34683	3.81242
n-1	8	8	8	n-1	8	8	8	n-1	8	8	8
CI_min	3.5019	3.7607	46.506		1.1056	1.1895	39.849		5.7297	4.12875	52.6218
CI_max	3.8315	4.1571	50.548		1.8358	1.801	45.535		6.4257	4.82241	60.2467
Eagle and SPOT-ELM					Eagle and SPOT- ATCOR						
Abs diff	-2.196	-2.4636	-5.8351		Abs diff	2.411	0.5167	7.9076			
Rel diff	-59.89	-62.23	-12.024		Rel diff	65.755	13.051	16.2954			

GRASS OFF-NADIR											
	Eagle				SPOT-ELM				SPOT-ATCOR		
	SPOT1	SPOT2	SPOT3		SPOT1	SPOT2	SPOT3		SPOT1	SPOT2	SPOT3
$\overline{x}$	2.6389	3.09	33.983		2.5512	2.3672	34.351	$\overline{x}$	7.1172	5.60486	44.7843
SD	0.2305	0.3455	1.5723	SD	0.3423	0.3398	1.0318	SD	0.3423	0.38163	1.39475
SE	0.0768	0.1152	0.5241	SE	0.1141	0.1133	0.3439	SE	0.1141	0.12721	0.46492
t	2.306	2.306	2.306	t	2.306	2.306	2.306	t	2.306	2.306	2.306
(t x SE)	0.1771	0.2656	1.2085	(t x SE)	0.2631	0	0.7931	(t x SE)	0.2631	0.29335	1.0721
n-1	8	8	8	n-1	8	8	8	n-1	8	8	8
CI_min	2.4617	2.8244	32.775		2.2881	2.3672	33.558		6.8541	5.31151	43.7122
CI_max	2.816	3.3556	35.192		2.8143	2.3672	35.144		7.3803	5.8982	45.8564
Eagle and SPOT-ELM					Eagle and SPOT- ATCOR						
Abs diff	-0.0877	-0.7228	0.3678		Abs diff	4.4783	2.5149	10.8009			
Rel diff	-3.3217	-23.39	1.0823		Rel diff	169.7	81.387	31.7831			

GRASS NEAR-NADIR											
	Eagle				SPOT-ELM				SPOT-ATCOR		
	SPOT1	SPOT2	SPOT3		SPOT1	SPOT2	SPOT3		SPOT1	SPOT2	SPOT3
$\overline{x}$	2.67	3.0878	34.408		2.0963	2.1492	34.922	$\overline{x}$	6.72	5.36842	45.5156
SD	0.3856	0.531	1.8905	SD	0.2559	0.2358	1.587	SD	0.2287	0.24581	2.13259
SE	0.1285	0.177	0.6302	SE	0.0853	0.0786	0.529	SE	0.0762	0.08194	0.71086
t	2.306	2.306	2.306	t	2.306	2.306	2.306	t	2.306	2.306	2.306
(t x SE)	0.2964	0.4081	1.4532	(t x SE)	0.1967	0.1812	1.2199	(t x SE)	0.1758	0.18894	1.63925
n-1	8	8	8	n-1	8	8	8	n-1	8	8	8
CI_min	2.3736	2.6796	32.955		1.8996	1.968	33.703		6.5442	5.17948	43.8764
CI_max	2.9664	3.4959	35.861		2.293	2.3305	36.142		6.8958	5.55737	47.1549
Eagle and SPOT-ELM					Eagle and SPOT- ATCOR						
Abs diff	-0.5737	-0.9385	0.5146		Abs diff	4.05	2.2806	11.1078			
Rel diff	-21.488	-30.395	1.4956		Rel diff	151.69	73.86	32.2829			